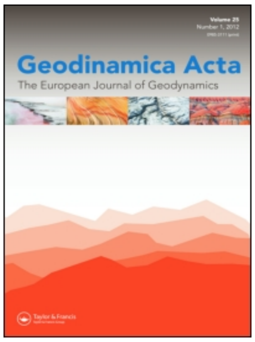

Taylor & Francis
Taylor & Francis Group

Geodinamica Acta

ISSN: 0985-3111 (Print) 1778-3593 (Online) Journal homepage: https://www.tandfonline.com/loi/tgda20

Age and Chemistry of Miocene Volcanic. Rocks from the Kiraz Basin of the Küçük Menderes Graben: Its Significance for the Extensional Tectonics of Southwestern Anatolia, Turkey'

Erdin Bozkurt , John A. Winchester , Gilles Ruffet & Bora Rojay

To cite this article: Erdin Bozkurt , John A. Winchester , Gilles Ruffet & Bora Rojay (2008) Age and Chemistry of Miocene Volcanic. Rocks from the Kiraz Basin of the Küçük Menderes Graben: Its Significance for the Extensional Tectonics of Southwestern Anatolia, Turkey', Geodinamica Acta, 21:5-6, 239-257, DOI: 10.3166/ga.21.239-257

To link to this article: https://doi.org/10.3166/ga.21.239-257

Published online: 13 Apr 2012.

Geodinamica Acta

Geodinamica Acta 21/5-6 (2008) 239-257

Age and Chemistry of Miocene Volcanic. Rocks from the Kiraz Basin of the Küçük Menderes Graben: Its Significance for the Extensional Tectonics of Southwestern Anatolia, Turkey'

Erdin Bozkurt[1*], John A. Winchester[2], Gilles Ruffet[3, 4] & Bora Rojay[1]

[1] *Department of Geological Engineering, Middle East Technical University, TR–06531 Ankara, Turkey*

[2] *Earth Science & Geography, School of Physical & Geographic Sciences, Keele University, Staffordshire ST5 5BG, England*

[3] *CNRS (CNRS/INSU) UMR 6118, Géosciences Rennes, 35042 Rennes Cedex, France*

[4] *Université de Rennes 1, Géosciences Rennes, 35042 Rennes Cedex, France*

Received: 22/05/2008, accepted: 29/12/2008

Abstract

Neogene volcanic rocks and granitoid plutons are among the most important geological components of western Turkey. Although they are voluminous north of the Gediz Graben, they are very scarce to the south, where volcanic rocks occur as isolated small exposures in a small number of localities. The Kiraz Basin of the Küçük Menderes Graben is a key locality, in which Tertiary volcanic rocks crop out at three locations. These rocks have been chemically analysed and dated (^{39}Ar-^{40}Ar whole rock and biotite analyses) in order to understand their tectonic setting of emplacement and its relation to the wider structure of western Anatolia. Whole rock and biotite ^{39}Ar-^{40}Ar ages vary between 13.9 ± 0.2 Ma and 14.6 ± 0.2 Ma.

The Kiraz volcanic rocks are calc-alkaline, with a compositional range from basaltic andesite to dacite. They are strongly enriched in the light ion lithophile elements (LILE) and have chemistries typical of lavas erupted in subduction-related settings. Their close association with rift-bounding faults suggests eruptions via conduits flanking grabens in an extensional environment. The difference in chemical composition and age between the Kiraz volcanic rocks and the slightly older calc-alkaline volcanic rocks north of the Gediz Graben is attributed to their relatively younger ages and greater proximity to the Aegean Arc. Their calc-alkaline chemistry reflects magma generation influenced by the slab descending beneath this arc and eruption/emplacement in an extensional setting.

Keywords: Neogene volcanism, continental extension, ^{39}Ar-^{40}Ar dating, geochemistry, slab decent, Southwestern Anatolia, Turkey

1. Introduction

Western Turkey is currently experiencing north–south continental extension (e.g., [1–5]) (Fig. 1). Its Tertiary evolution is characterized by core-complex evolution and basin formation, normal faulting and graben formation, and coeval intrusive and extrusive magmatic activity. The Menderes Massif and east–west- trending grabens form the major features of the region. The massif has been exhumed in the footwall of presently low-angle normal faults (detachment faults) in

* Corresponding author.
Email address : erdin@metu.edu.tr

doi:10.3166/ga.21.239-257

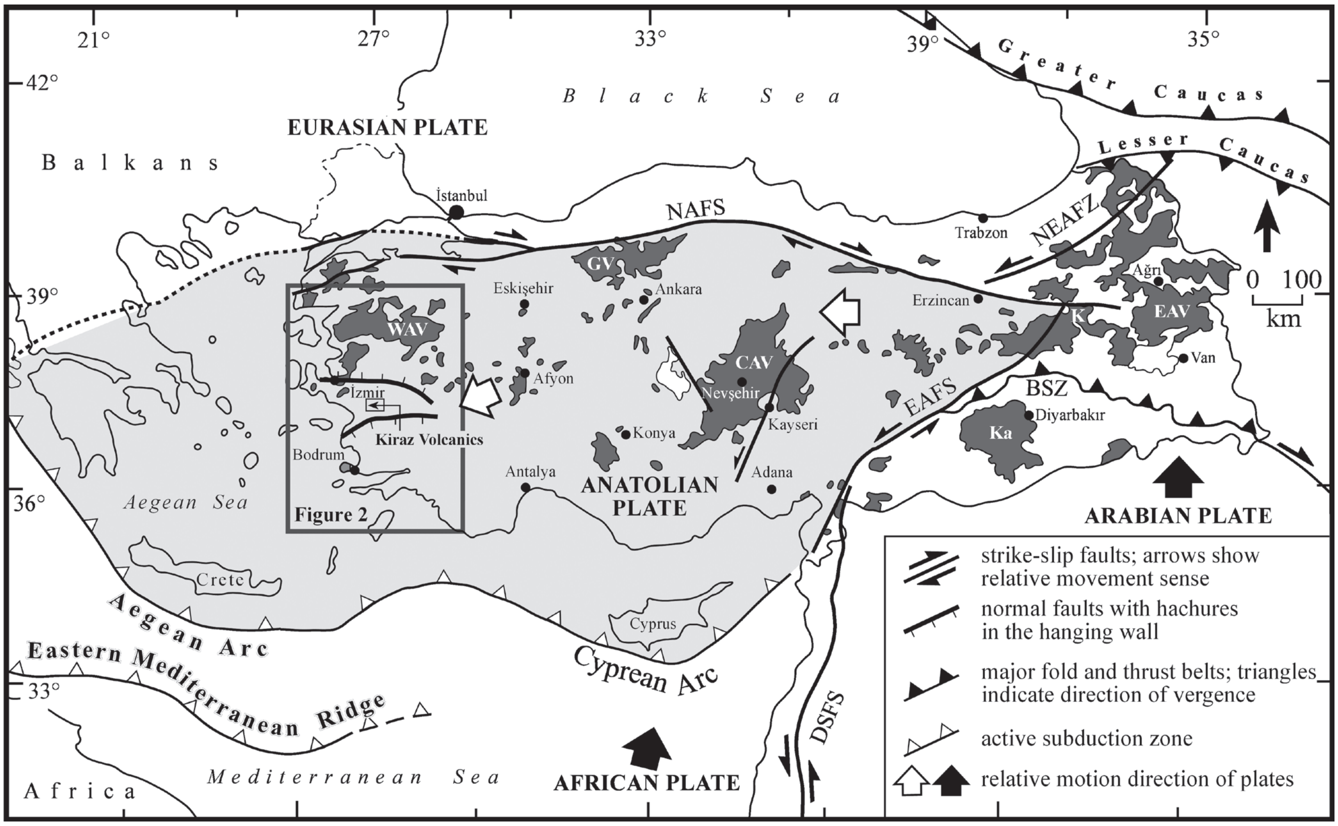

Fig. 1: Simplified geological map showing neotectonic elements and the location of the main Tertiary–Quaternary volcanic provinces of Turkey and nearby regions (compiled and modified from [2, 3, 114, 115]). BSZ– Bitlis Suture Zone; CAV– Central Anatolian Volcanic Province; EAFS– East Anatolian Fault System; EAV– Eastern Anatolian Volcanic Province; GV– Galatia Volcanic Province; K– Karlıova; Ka– Karacadağ volcano; NAFS– North Anatolian Fault System; WAV– Western Anatolian Volcanic Province.

whose hanging walls synchronous continental red clastic sediments were deposited. It comprises three distinct submassifs, bounded by active ~E–W-trending grabens, namely the northern (Gördes), central (Ödemiş-Kiraz) and southern (Çine) submassifs. Core-complex formation of each submassif was diachronous, commencing between late Oligocene to early Miocene time. The Gediz and the Büyük Menderes grabens are the best studied E–W-trending grabens and they bound Menderes submassifs. Initiated in latest Miocene to Pliocene time, they are flanked by high-angle normal faults, many of which are still active, capable of producing devastating earthquakes, and therefore much studied (e.g., [6–11]). Apart from its tectonic importance, Western Anatolia is also well studied because of widespread Neogene volcanism (e.g., [12–18] and references therein), extensive mineralization (e.g., [19–21]) and geothermal systems (e.g., [22] and references therein) accompanying the continental extension.

The origin and age of continental extensional tectonics in western Anatolia formed the subject of intense research over the last three decades. Four alternative models have been proposed: (i) back-arc extension consequent to southwestward subduction roll-back along the Aegean-Cyprian arc system (e.g., [23–26]); (ii) tectonic westward escape of Anatolian microplate along dextral North Anatolian and sinistral East Anatolian fault systems (EAFS and NAFS) [2, 27, 28]; (iii) post-orogenic collapse of the crust [29] over-thickened during the closure of the northern Neotethys [30, 31]; (iv) rapid southwestward movement of Greece relative to Anatolia [32]. The onset age of extension in these models varies greatly between 5 to 60 Ma. The recent literature now agrees that the extension commenced by the latest Oligocene–early Miocene time and is represented by (i) and early phase of core-complex formation in the footwall of presently low-angle normal faults (latest Oligocene–Miocene orogenic collapse and back-arc extension) and (ii) Plio–Quaternary modern phase of graben formation along high-angle normal faults (combined effect of tectonic escape and subduction roll-back processes). However, it is still debated if the distinct styles evolved in a continuous manner without any break (e.g., [33–36]) or in an episodic manner with more than one phases of extension separated by phases of contraction and/or tectonic quiescence (e.g., [3, 4, 37–52]). A detailed information on these issues lie outside the scope of this paper, and for further information the readers are referred to a number of recent publications (e.g., [36, 40–43, 50, 51, 53–57] and references therein).

Western Anatolia is also characterized by extensive Neogene magmatism; there are temporal and spatial relationships between volcanic and plutonic activity. Lava flows of varied compositions, pyroclastics and genetically associated hypabyssal rocks are widespread; granitoid plutons are

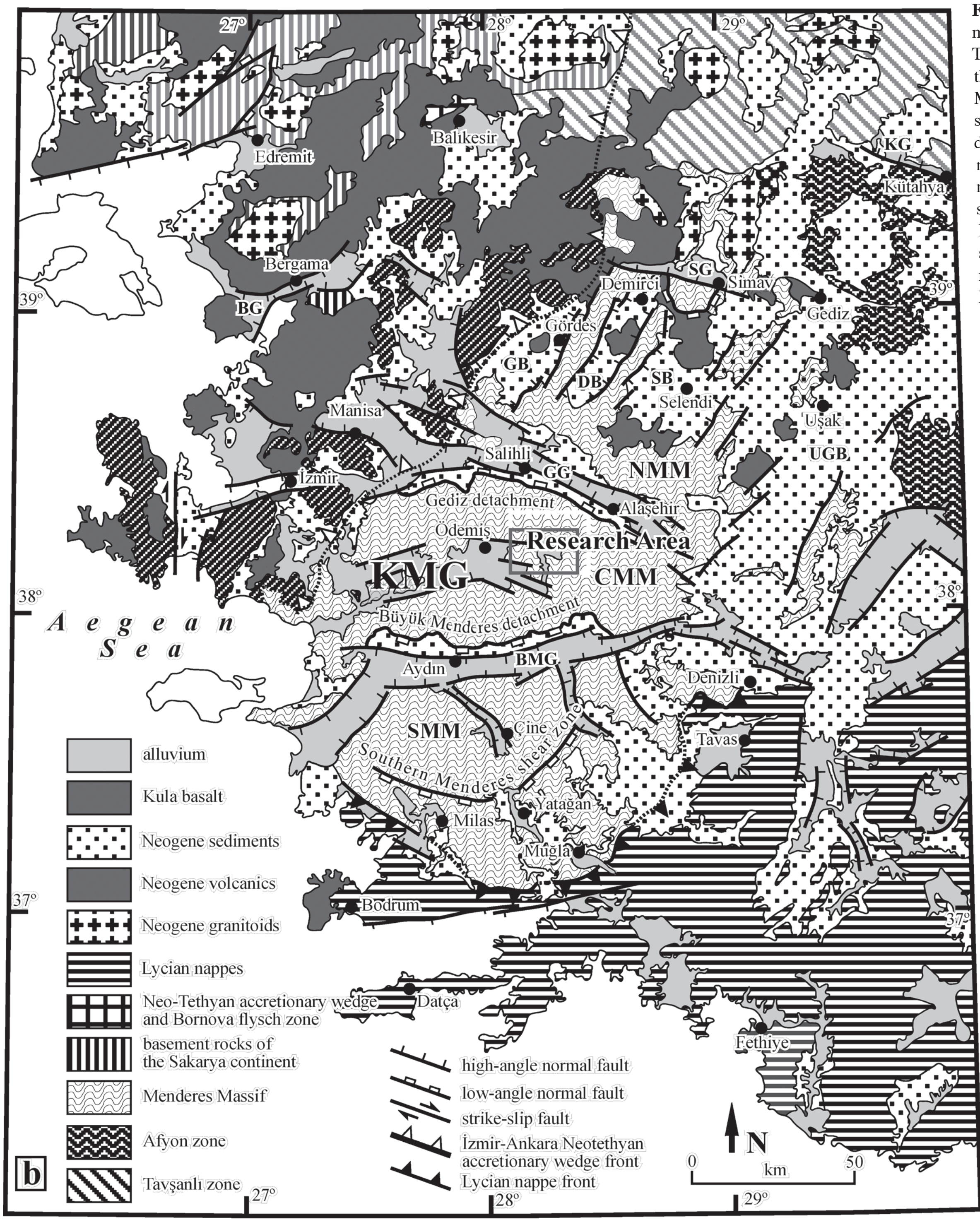

Fig. 2: Geological map of western Turkey showing the Menderes Massif and its subdivision. The distributions of rock units are modified and simplified from MTA 1:500 000-scale geological maps, İzmir and Denizli sheets. **BG**– Bakırçay Graben; **DB**– Demirci Basin; **GB**– Gördes Basin; **GG**– Gediz Graben; **KG**– Kütahya Graben; **SB**– Selendi Basin; **SG**– Simav Graben; **BMG**– Büyük Menderes Graben; **CMM**– Central Menderes Massif; **KMG**– Küçük Menderes Graben; **NMM**– Northern Menderes Massif; **SMM**– Southern Menderes Massif; **UGB**– Uşak-Güre Basin.

also common. Magmatic activity occurred in four distinct episodes in the Eocene (e.g., [12, 13, 15–18, 45, 58–60]), latest Oligocene–Middle Miocene, Late Miocene and latest Pliocene–Quaternary times, and is most voluminous north of the Gediz Graben. Eocene volcanic rocks also occur as small exposures in the Biga Peninsula. In contrast, Tertiary volcanic rocks are very scarce to the south of the Gediz Graben (Fig. 2). The characteristics of the magmatic rocks produced during these phases are summarized below:

(1) Eocene magmatism was limited mostly to the northernmost part of western Anatolia along the southern margin of Marmara Sea and is represented mostly by shallow-crustal granitic plutons and their volcanic equivalents (e.g., [61] and references therein). Granitic plutons (~53–34 Ma: [61, 62] and references therein) are subalkaline, medium- to high-K monzogranite, granodiorite, and granite in composition. Volcanic equivalents consist of subalkaline basaltic to andesitic lavas (medium- to high-K series to shoshonites) and

associated pyroclastic rocks. They are attributed to a partial melting of subduction-enriched subcontinental lithospheric mantle and assimilation and fractional crystallization. The readers are refereed to recent papers for further reading ([61, 63] and references therein).

(2) Latest Oligocene–Middle Miocene (24–14 Ma) rocks are represented by intermediate to acidic lavas (dacitic to rhyolitic) and pyroclastics (rhyolitic to dacitic ignimbrite) within volcano-sedimentary sequences that fill many basins. They are intruded by widespread, genetically associated lava domes and abundant dyke swarms. Their chemistry is mainly subalkaline, medium- to high-K calc-alkaline and shoshonitic. The magma generation is attributed to partial melting of subduction-enriched subcontinental lithospheric mantle and assimilation and fractional crystallization; while the subduction component decreased with time, and the degree of crustal contamination increased ([61, 63] and references therein). Alternatively, the magmas might have been generated in the mantle wedge, not in the lithosphere (e.g., [60]). This magmatism was overlapped with continued regional compression and the development of a thick orogenic crust following the closure of the Neotethyan ocean; while melt generation was influenced by asthenospheric heat and slab break-off ([61, 63] and references therein). This time is also characterized by extensive granitoid plutonism at shallow crustal levels (e.g., the Kozak, Evciler and Alaçam granitoids) (e.g., [12, 13, 16–18, 31, 60, 64–83]). Crustal thickening was followed by crustal extension resulting from a combination orogenic collapse and southward rollback of the Aegean subduction zone; regional extension commenced by the latest Oligocene–Early Miocene period. Metamorphic core-complex formation and consequent exhumation of the Menderes Massif in the footwall of now low-angle normal faults commenced during this phase. The footwall deformation was locally associated with syn-extensional granitoid emplacement (e.g., the Eğrigöz, Koyunoba, Turgutlu and Salihli granitoids: [36, 84–88]). With the passage of time, volcanic activity became more alkaline with decreasing crustal contamination and subduction influence but an increasing contribution of asthenospheric mantle-derived melts.

(3) Following a period of volcanic quiescence lasting from c. 14 to 12 Ma, local rift-related alkaline magmatism (alkali basalt lavas, basanites and tephrites) resumed in discrete locations in the region. The magma generation is mainly attributed to decompressional melting of the asthenospheric mantle where magmas have no component of subduction and crustal contamination ([61, 62] and references therein). Some of these basalts have also mixed orogenic-intraplate signature [89]. Graben-bounding high-angle normal faults acted as conduits for the magma to reach the surface (e.g., [16–18, 61, 63, 69, 80, 90–96]). Many recent publications also give detailed information about the magmatic activity north of the Gediz Graben (e.g., [4, 15, 32, 45, 92] and references therein).

(4) From latest Pliocene (1.94±0.16 Ma) till Quaternary pre-historic time (0.13±0.05 Ma) sodic alkaline basaltic volcanism from Kula represents the last phase of volcanic activity in western Turkey (e.g., [14, 90, 97–99]).

Whereas Oligocene to Miocene potassic volcanic rocks are abundant on the Biga Peninsula and in areas of Anatolia further to the east, south of the Gediz Graben small extrusions of middle Miocene volcanic rocks occur associated with the Küçük Menderes Graben (Fig. 2). At the eastern end of this graben is an almost detached fault-bounded basin, the Kiraz Basin, which is an approximately 30-km-long, 1–15-km-wide depression trending NW–SE separated from the main Küçük Menderes Graben by a topographic high [47, 50, 53].

Within the Kiraz Basin Tertiary volcanic rocks have been observed in three locations, east, northeast and south of the town of Kiraz (Fig. 3). Because the contrast in abundance of volcanic rocks north and south of the Gediz Graben is so striking, it was considered necessary to sample the rare volcanic rocks in the Kiraz Basin in order to establish any chemical contrasts and hence to understand the tectonic implications of these contrasts in terms of the structure of western Anatolia.

Approximately 1 km east of Kiraz, around the village of Karaburç, basaltic andesites crop out over an area of several hundred m^2, resting unconformably upon and locally seen to intrude schists of the Menderes Massif. They are overlain unconformably by Pliocene red clastic sedimentary rocks. Their age is therefore constrained as pre-Pliocene, but they postdate the Eocene metamorphism that affected the schist envelope of the Menderes Massif. Around the village of Yenişehir, about 2 km SSE of Kiraz, andesitic volcanic rocks crop out. These also rest unconformably on schists of the Menderes Massif and are themselves largely obscured by Quaternary alluvial fan deposits: the outcrop area is barely more than one hectare. Field evidence suggested that these rocks are likely to be similar in age to the volcanic rocks around Karaburç. Finally, approximately three kilometres northeast of Kiraz, in the Bozdağı mountains, intrusive subvolcanic dykes of andesitic to dacitic composition also form small exposures (too small to map at a 1/25000 scale) in the Başova area. They cut and are emplaced into both schists and augen gneisses of the Menderes Massif: no associated extrusive rocks were observed. Their field relationships, however, suggest that these rocks may have been feeder dykes for a similar volcanic centre and also form part of the same magmatic province.

2. Kiraz Basin: Established Knowledge

The basin floor of the Kiraz Basin lies about 250 m above sea level. It is bounded by active high-angle normal faults at its northeastern and southwestern margins, suggesting that it is an actively subsiding graben. Its geology was the subject of recent research as it is important in understanding better the extensional tectonics in western Anatolia [47, 50, 53, 100, 101].

The basin fill is composed of Neogene continental red clastics to lacustrine sediments and associated volcanic rocks that developed above the metamorphic rocks of the Menderes Massif. The basement is composed mainly of schists, quartzites,

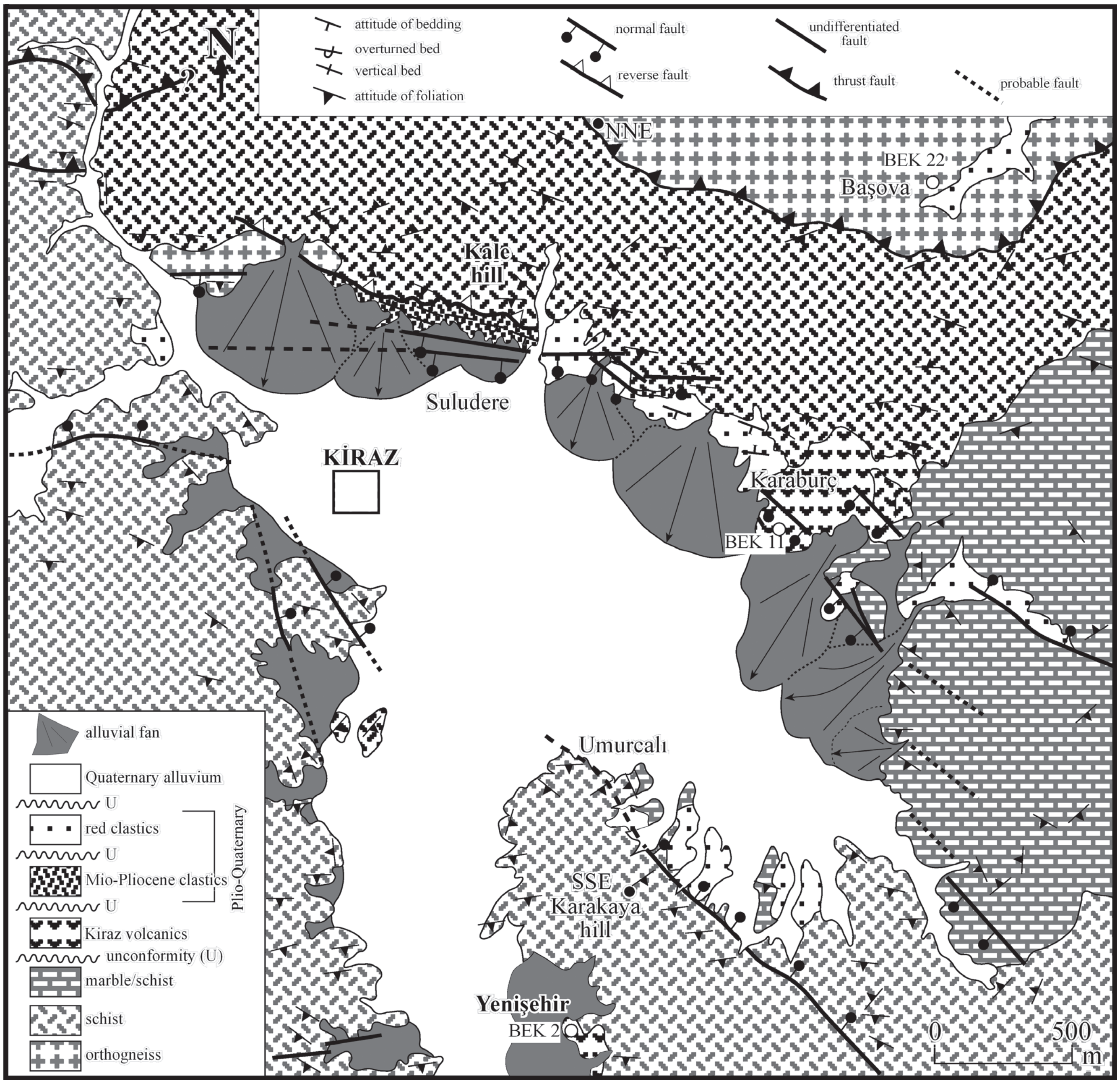

Fig. 3: Simplified geological map of the Kiraz Basin (from [47]). BEK2, 11 & 22 shows the location of samples dated with ^{39}Ar-^{40}Ar laser probe.

phyllites, marbles and orthogneisses (traditionally known as augen gneisses). The Neogene basin fill comprises two distinct lithologic associations: (i) lower (older) beige-light green to grey-dirty white-light brown well-bedded clastic to lacustrine rocks and (ii) upper (younger) poorly bedded red continental clastic rocks. The first group of rocks (Suludere formation of Emre *et al.* [101]) is exposed and exhumed only along the north-eastern margin of the basin while the younger rocks crop out along both margins. The older Neogene sediments are deformed (tilted almost to vertical with dips ranging from 40° and 89°) and even overturned, particularly near their contact with the metamorphic rocks along the northeastern margin of the basin. Bozkurt and Rojay [2005] argued for an Early Miocene–Early Pliocene age for these sediments but Emre and his colleagues [101] later demonstrated, based on fresh-water ostracoda, a latest Middle Miocene–Late Miocene age. The fossil content is in agreement with the isotopic age of the volcanic rocks (Emre and Sozbilir [100] and this study), since the lowermost coarse clastic rocks (conglomerates) contain fragments derived from the underlying volcanic rocks. Younger clastic rocks (Aydoğdu formation of Emre *et al.* [101]) unconformably overlie the basement and older Neogene sediments. They comprise an alternation of poorly bedded to semi-lithified conglomerate, sandstone and claystone, while coarse clasts include abundant andesitic fragments derived from the Neogene volcanics of the Kiraz Basin. As this formation is undeformed, indicated by its

Table 1: Whole-rock analyses of Kiraz volcanics. Abbreviations: **and**– andesite; **bas and**– basaltic andesite; **dac**– dacite.

Sample	BEK1	BEK2	BEK3	BEK4	BEK5	BEK6	BEK7	BEK9	BEK10	BEK11
rock type	bas and	bas and	bas and	bas and	bas and	bas and	bas and	andesite	andesite	andesite
locality	Yenişehir	Yenişehir	Yenişehir	Yenişehir	Yenişehir	Yenişehir	Yenişehir	Karaburç	Karaburç	Karaburç
SiO2	54,56	54,71	53,36	53,40	54,97	53,47	54,12	58,08	57,97	60,03
TiO2	0,85	0,89	0,90	0,89	0,85	0,78	0,88	0,82	0,84	0,77
Al2O3	15,54	15,85	14,97	15,30	15,94	14,51	15,80	16,01	15,68	15,11
Fe2O3T	7,10	6,77	6,74	7,07	6,67	6,80	6,93	6,42	6,63	6,01
MnO	0,12	0,12	0,13	0,13	0,12	0,13	0,13	0,10	0,11	0,10
MgO	5,04	3,74	4,48	4,21	4,70	4,08	4,16	2,16	5,12	4,51
CaO	9,12	8,19	7,59	7,86	7,20	8,46	7,39	7,03	6,77	6,19
Na2O	2,91	2,64	2,77	3,06	2,88	2,72	2,99	2,76	3,09	3,48
K2O	1,37	1,37	1,41	1,54	1,56	1,41	1,57	2,16	1,57	2,08
P2O5	0,15	0,14	0,15	0,16	0,17	0,14	0,17	0,19	0,18	0,17
LOI	2,83	5,36	6,94	5,89	4,43	7,47	5,46	3,67	1,54	0,95
Total	**99,60**	**99,79**	**99,45**	**99,52**	**99,50**	**99,98**	**99,61**	**99,41**	**99,51**	**99,41**
Ba	341	329	362	390	383	365	349	700	725	630
Cl	34	63	15	11	23	19	17	15	46	90
Cr	167	249	232	225	249	229	218	170	184	189
Cu	32	28	24	23	22	23	22	23	18	20
Ga	18	18	19	17	20	18	19	20	21	19
Nb	9	10	10	11	11	9	10	11	10	11
Ni	35	36	28	24	21	28	18	32	42	38
Pb	19	14	12	16	13	17	11	47	45	39
Rb	47	50	48	57	56	56	58	41	40	72
Sr	457	397	373	388	383	382	395	402	502	497
Th	7	4	7	6	6	5	5	15	14	10
V	139	166	143	126	114	128	131	43	105	100
Y	24	25	24	22	24	22	22	16	22	22
Zn	69	67	63	64	65	60	63	64	77	69
Zr	153	155	145	147	159	128	145	179	180	173
La	18	25	28	19	32	22	23	40	38	33
Ce	21	52	15	37	18	44	48	35	60	55
Nd	17	30	19	27	10	27	29	8	26	28
S	0,01	0,01	0,01	0,01	0,01	0,01	0,01	0,01	0,01	0,01

gently inclined and/or horizontal attitudes, it has been assigned a Plio–Pleistocene age [47, 50, 101]. The Quaternary alluvium (marginal alluvial fans and graben floor sediments) forms the youngest lithologic association in the Kiraz Basin. Neogene volcanics will be discussed in the following section.

Three distinct structural elements played important roles in the evolution of the Kiraz Basin: (i) a WNW–ESE-trending, north-facing high-angle oblique-slip reverse fault, along which the metamorphic rocks of the Menderes Massif are thrust on to the older Neogene clastic sediments along the northeastern margin of the basin. This structure provides the first ever evidence about the presence of Neogene thrusting in western Turkey that supports episodic two-stage extension with an intervening short-term phase of contractional

BEK12	BEK13	BEK14	BEK15	BEK16	BEK17	BEK18	BEK19	BEK20	BEK21	BEK22	BEK23
andesite	andesite	andesite	andesite	andesite	andesite	dac dyke	and dyke	dac dyke	and dyke	dac dyke	and dyke
Karaburç	Karaburç	Karaburç	Karaburç	Karaburç	Karaburç	Bozdağ	Bozdağ	Bozdağ	Bozdağ	Bozdağ	Bozdağ
59,51	60,97	61,11	61,88	61,17	61,68	63,93	62,44	63,99	59,82	63,41	60,87
0,82	0,76	0,80	0,81	0,78	0,86	0,74	0,77	0,89	0,79	0,71	0,76
15,16	15,30	15,33	15,00	15,10	15,62	16,17	17,55	18,17	15,14	15,96	15,95
6,35	6,28	6,18	5,99	6,24	6,61	5,18	5,31	2,56	5,42	5,01	5,17
0,10	0,11	0,09	0,10	0,10	0,10	0,08	0,07	0,02	0,08	0,08	0,13
4,86	3,38	3,56	4,39	3,52	1,89	0,86	0,88	0,83	2,59	2,31	2,07
6,46	5,68	5,91	5,73	6,06	4,91	5,15	5,60	5,69	6,07	5,78	6,06
2,99	3,06	3,06	3,04	3,15	2,83	3,13	3,50	3,39	3,34	2,92	2,94
2,06	2,40	2,45	2,19	2,46	2,77	2,42	2,62	2,71	2,53	2,36	2,39
0,18	0,17	0,19	0,17	0,18	0,18	0,15	0,16	0,17	0,15	0,15	0,15
1,11	1,44	0,88	0,70	0,70	2,09	1,89	1,61	1,08	3,47	1,39	3,07
99,61	**99,56**	**99,59**	**100,01**	**99,47**	**99,55**	**99,71**	**100,52**	**99,51**	**99,41**	**100,09**	**99,57**
636	639	804	619	595	624	525	553	519	494	479	471
73	24	45	16	12	22	90	67	65	63	68	67
178	206	213	182	191	220	98	89	107	156	117	113
19	24	21	25	22	21	10	14	11	14	15	13
19	20	18	18	20	19	21	20	21	20	20	17
11	10	10	11	11	10	10	11	11	10	11	10
34	49	37	37	42	39	10	11	7	12	11	11
47	45	40	37	36	44	36	34	28	31	35	32
64	79	82	71	81	88	93	96	97	91	91	92
510	468	485	467	477	399	392	399	388	374	385	362
13	14	13	10	17	13	11	8	11	9	14	13
94	100	125	80	96	64	92	86	107	81	80	78
24	24	23	24	23	23	26	25	19	22	24	23
70	69	72	71	70	69	70	66	49	67	65	73
182	174	184	179	170	190	171	173	191	172	164	161
39	52	42	33	38	36	29	21	35	37	19	23
88	62	74	77	51	71	62	50	84	53	48	24
36	27	38	41	22	32	29	27	46	28	20	12
0,01	0,01	0,03	0,01	0,01	0,01	0,01	0,01	0,01	0,01	0,01	0,01

deformation [47, 50]. (ii) The older Neogene sediments are deformed into an overturned syncline with an almost WNW–ESE-trending fold axis paralleling the reverse fault. This feature is attributed to a fault-forced structure, with its northern limb overturned [47]. (iii) Margin-bounding high-angle (~40°) normal faults form a third group of structures that bounds and controls the Kiraz Basin.

3. Neogene Volcanics: Field Relations and Petrography

Neogene volcanics form another conspicuous element of the Kiraz Basin, although limited in extent, as described above. They were previously studied by Emre and Sözbilir [100] who described the geochemical characteristics of a small sample of these rocks. These authors also provided the first

^{39}Ar-^{40}Ar ages from two exposures near Yenişehir (14.3±0.1 Ma) and Başova (14.7±0.1 Ma), but is not clear whether the data are mineral or whole rock ages.

Porphyritic basaltic andesites, exposed in a small outcrop immediately southeast of Yenişehir village, are characterisitically greenish grey to dark grey when fresh, but are locally kaolinitized. Large plagioclase and mafic phenocrysts in a fine-grained matrix can readily be recognized at outcrop scale. Where weathering is severe, exfoliation with circular outlines and reddish-brownish to pinkish discolouration is characteristic. In this particular locality, the porphyritic rocks cut both the regional foliation and associated mineral stretching lineation in the metasediments. The phenocrysts are mainly plagioclase and rare pyroxene and hornblende; the matrix is fine-grained and composed mainly of plagioclase microlites, with smaller amounts of hornblende, pyroxene (rare) and volcanic glass. Plagioclase phenocrysts are bimodal in size: there are very large zoned euhedral crystals and relatively small ones displaying mainly albite and/or Carlsbad twinning; the latter group commonly occur as laths but do not show any preferred orientation. Clusters of different sizes of plagioclase phenocrysts, enclosed by fine-grained matrix, define a well-developed glomeroporphyritic texture in many of the samples. Albite twins taper towards the edge of phenocrysts. Other microstructures such as undulose extinction and deformation bands/lamellae, may indicate deformation of early crystals during the subsequent magma flow. Plagioclases may be kaolinitized and seritized. Pyroxene and hornblende also occur as phenocrysts but they are smaller than the plagioclases. Hornblende usually occur as blades whereas pyroxenes form euhedral equidimensional crystals.

Light grey to pinkish-purple porphyritic andesites exposed west of Karaburç occur as either lava flows or high-level dykes or volcanic necks. The lava flows show characteristic flow texture. These volcanics share similar microfabrics. In addition to plagioclase and hornblende, biotite occurs as phenocrysts. The hornblende is more abundant and forms either large six-sided euhedral crystals or blades; some of which show two well-developed sets of cleavage at 120º angles. Black opaque minerals characteristically rim hornblende and biotite. Replacement textures are common; there are examples of ghost hornblende crystals, replaced by a chlorite and opaque mineral aggregate. Glomeroporphyritic texture defined by clusters of hornblende phenocrysts is also characteristic. Biotite is very common and sometimes forms very large phenorcrysts. Pyroxene is rare. The relative abundance of phenocrysts is greater in rocks from volcanic necks than in lava flows. The matrix in the lava flows is dominated by volcanic glass with smaller amounts of oriented plagioclase microlites, hornblende and biotite crystals. In contrast, the matrix of rock samples from the volcanic neck is composed mainly of plagioclase microlites. Carbonate replacement is common both in the matrix and hornblende phenocrysts.

The exposures south of Başova are microgranite to porphyritic andesite/dacite. Large biotite, hornblende and plagioclase phenocrysts within a grey to pinkish matrix are essential components; if altered, the colour of rock becomes reddish. They occur mainly as dykes intruding the orthogneisses; thin baked zones around their margins are readily seen in some exposures. Emre and Sözbilir [50, 100] mapped these rocks as a single body, but we found that they occur as small discrete exposures. Petrographically, they are very similar to volcanic rocks near Karaburç, except that biotite is the most abundant phenocryst phase. Green and brown pleochroism and very large biotite crystal sizes make these rocks appear very different from the other two areas of volcanic rocks. Biotite commonly has black opaque rims. Plagioclase crystals are typically zoned and characterized by intense alteration at the centre of each crystal.

Opaque phases, mainly magnetite, are very common in all three exposures. Alteration consists of extensive hematitization and calcitization of the groundmass.

4. Geochemistry

4.1. Analytical Procedure

Samples were obtained from all three areas for dating (10 kg) and geochemical analysis (1–2 kg). Extreme care was taken to get freshest, or least altered samples, free of veins. Numbers of samples reflect the availability of adequately fresh material from these small outcrops. Even so, enhanced LOI figures (Table 1) suggest that some alteration is present. Seven samples from Yenişehir, nine from Karaburç and six samples from Başova exposures for geochemical analysis. Twenty-one igneous rocks were analysed (Table 1) at Keele University, England, using an ARL 8420 X-ray Fluorescence spectrometer, calibrated against both international and internal Keele standards of suitable compositional range, as detailed in Floyd and Castillo [102]. Analytical methods and precision have been described in Winchester *et al*. [103].

4.2. Composition of Igneous Suites

A total alkali-silica (TAS) diagram [104] shows that the Küçük Menderes subalkaline volcanic rocks range in composition from basaltic andesite, through andesite to dacite, with a distinct break in composition between basaltic andesite and andesite (Fig. 4a). On this diagram the symbols for the analyses are separated according to the locality from which they were collected. Thus the basaltic andesites from Yenişehir, indicated by crosses, are distinguished from the Karaburç andesites (filled circles) and the dacitic and andesitic intrusives of the Bozdağı area (triangles).

Although these rocks are mostly fresh, because some showed incipient signs of alteration, they were also plotted on a SiO_2-Zr/TiO_2 diagram [105], which confirmed both their subalkaline chemistry and compositional range (Fig. 4b). However, a Zr/TiO_2-Nb/Y diagram (not plotted here) shows that there is no increase in Zr/TiO_2 content between the andesites and dacites, suggesting that the silica enhancement in the latter rocks is not matched by other chemical criteria: the likely

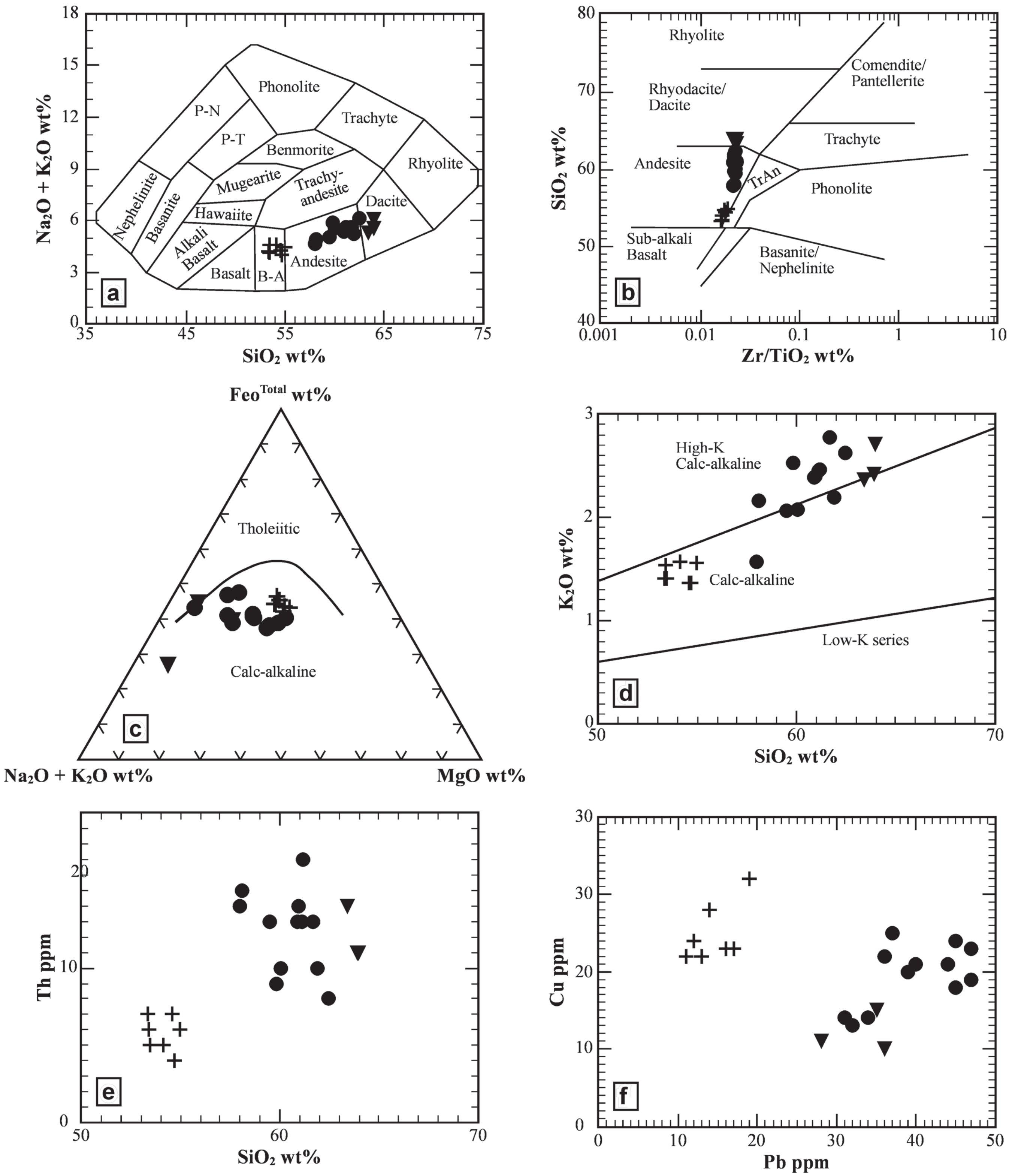

Fig. 4: **(a)** A total alkali-silica (TAS) diagram [104]; **(b)** SiO_2-Zr/TiO_2 diagram [105]; **(c)** ternary AFM diagram [106]; **(d)** K_2O-SiO_2 diagram [107]; **(e)** Th-SiO_2 diagram and **(f)** Cu-Pb diagram. Symbols: upright crosses– Yenişehir basaltic andesite, filled circles– Karaburç andesite, filled inverted triangles– Bozdağ dacite.

explanation is that some of these very small magmatic dykes were contaminated by silica from host-rocks as they were intruded. A ternary AFM diagram [106] also reveals the relative lack of iron enrichment, with all these rocks plotting as calc-alkaline, rather than tholeiitic (Fig. 4c). It also distinguishes chemically the rocks collected from the three different areas. However, the chemistry also raises doubts about whether all these rocks belong to a single magmatic suite.

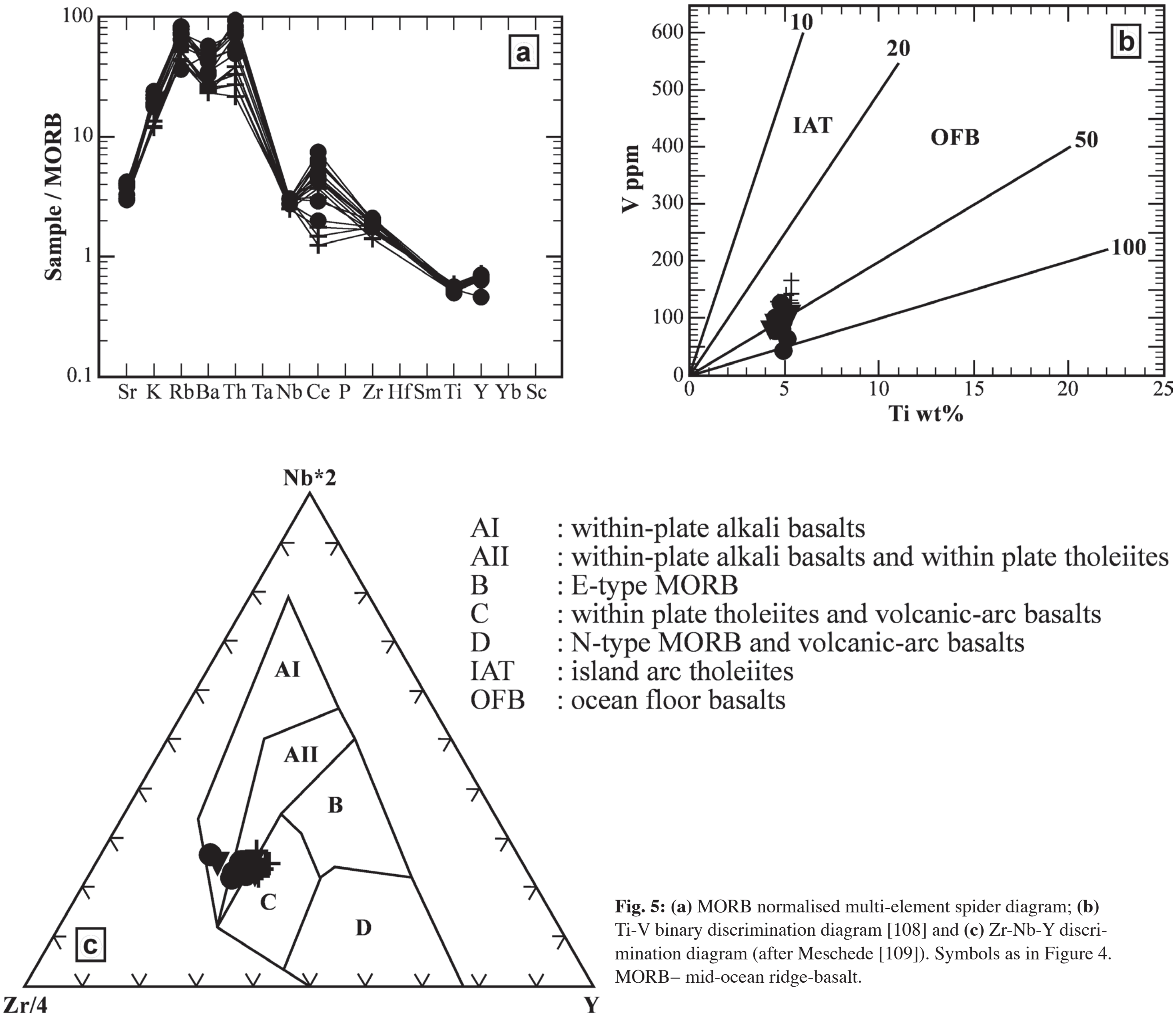

Fig. 5: (a) MORB normalised multi-element spider diagram; **(b)** Ti-V binary discrimination diagram [108] and **(c)** Zr-Nb-Y discrimination diagram (after Meschede [109]). Symbols as in Figure 4. MORB– mid-ocean ridge-basalt.

4.3. Discrimination Between Igneous Suites

As hinted above, the rocks collected from the three separate areas may be chemically distinguished. On a K_2O-SiO_2 diagram (Fig. 4d), using the field boundaries of Peccerillo and Taylor [107], whereas the basaltic andesites from Yenişehir all plotted in the calc-alkaline field, the bulk of the andesites and dacites plotted as part of a high-K calc-alkaline suite. This difference suggests that these rocks may not belong to a single magmatic suite, as they do not appear to fall on a single trend. Separation between the andesites (plus the dacites) and the basaltic andesites is clearly shown by a marked jump in Th content on a Th-SiO_2 diagram (Fig. 4e), suggesting again that they might in fact belong to quite discrete suites. This difference is also emphasized on a Cu-Pb diagram (Fig. 4f), elements whose compositional variation is less controlled by fractionation than Si or Th. This diagram shows most clearly the separation between the basaltic andesite suite from Yenişehir and the andesites and dacites from the other two locations which also occupy entirely separate fields.

4.4. Tectonic Setting Discrimination

On a multi-element spider diagram, normalised against MORB, while both suites are strongly enriched in the light ion lithophile elements (LILE), and also show the relative lack of enrichment in Nb typical of calc-alkaline suites, the greater enrichment of the andesitic suite distinguishes it from the basaltic andesites (Fig. 5a). All the samples have chemistries typical of mainstream calc-alkaline intermediate rocks. Their compositions are quite distinct from those of boninitic suites as they contain much lower MgO, Cr and Ni, so are unlikely to have been erupted in a forearc setting, but are typical of magmas erupted in either an island arc or an active continental margin setting or behind the crest of the magmatic arc. Such a setting is also indicated on a Ti-V binary plot [108] (Fig. 5b), in which all the magmas plot together in the ocean floor basalt field in an area which is also shared by calc-alkaline lavas. A Zr-Nb-Y ternary diagram [109] shows the basaltic andesites straddling the divide between the AII and C fields (Fig. 5c), effectively the range of within-plate tholeiites. Such a distribution might at first appear to contradict the findings of the Ti-V diagram, and yet it fits well the likely composition of magmas erupted via conduits flanking grabens in an extensional environment.

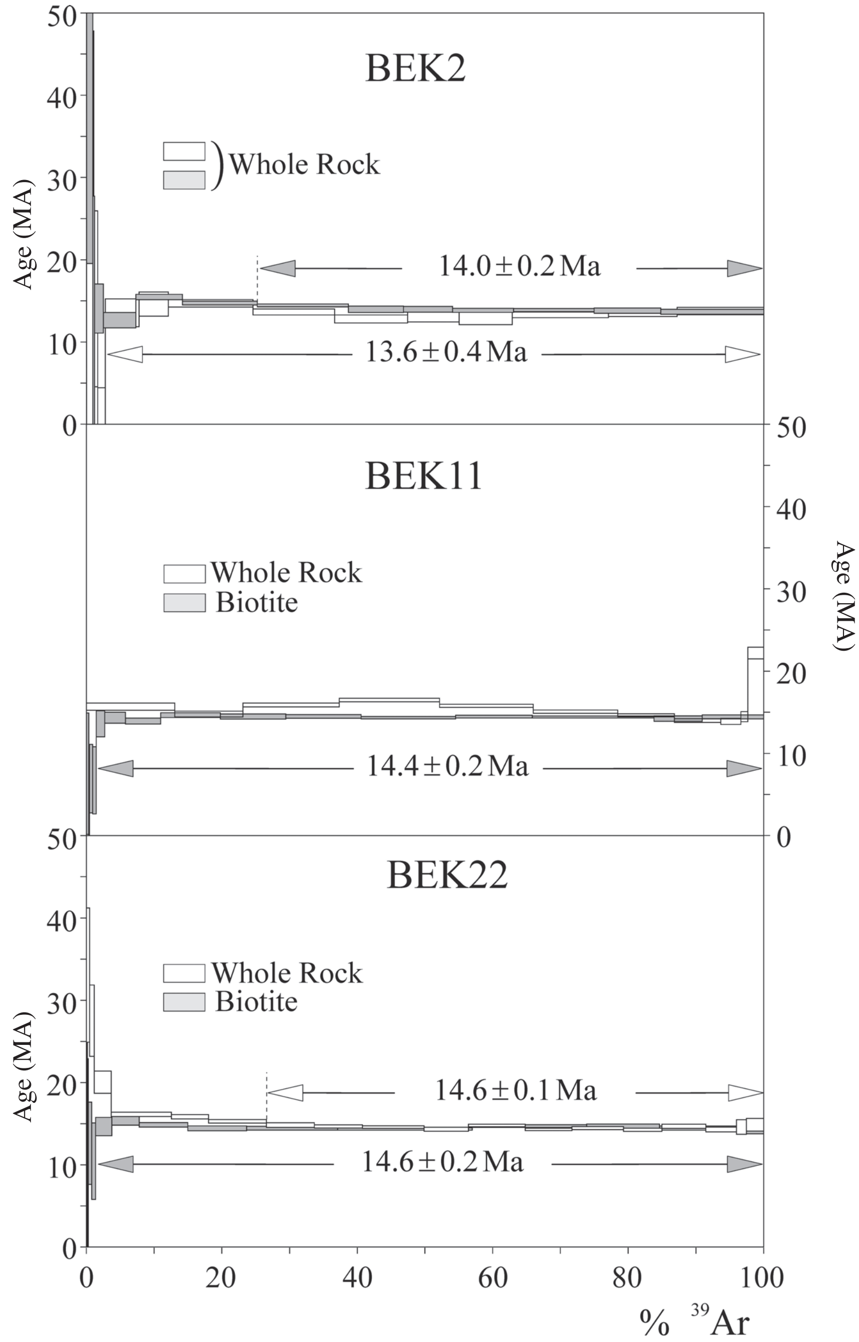

Fig. 6: ^{39}Ar-^{40}Ar age spectra of 3 samples of volcanic rocks from the Kiraz Basin. The age error bars for each temperature steps are at the 2σ level and do not include errors in the J-values. The errors in the J-values are included in the plateau age calculations.

5. ^{39}Ar-^{40}Ar Data

5.1. Analytical Procedure

Three samples (BEK 2, 11 and 22) were analyzed with an ^{39}Ar-^{40}Ar laser probe (CO_2 Synrad®). Analyses were performed on single whole-rock fragments from each sample with a duplicate for sample BEK2. Two analyses were also performed on biotite single grains from samples BEK 11 and 22 (see Figure 3 for location of samples).

Whole rock fragments and minerals were carefully hand picked under a binocular microscope from crushed rocks (0.3–2 mm fraction). The samples were wrapped in A1 foil to form packets (11 mm × 11 mm × 0.5 mm). These packets were stacked up to form a pile, within which packets of flux monitors were inserted every 8 to 10 samples. The stack, put in an irradiation can, was irradiated for 40 hours at the McMaster reactor (Hamilton, Canada) with a total flux of 5×10^{18} n.cm^{-2}. The irradiation standard was the sanidine TCR-2 (28.34 Ma according to Renne *et al.* [110]). The sample arrangement allowed us to monitor the flux gradient with a precision of ±0.2%.

The laser probe step-heating experimental procedure has been described in detail by Ruffet *et al.* [111, 112]. Blanks are performed routinely each first or third run, and are subtracted from the subsequent sample gas fractions. Analyses are performed on a MAP215® mass spectrometer.

To define a plateau age, a minimum of three consecutive steps are required, corresponding to a minimum of 70% of the total $^{39}Ar_K$ released, and the individual fraction ages should agree to within 1σ or 2σ with the integrated age of the plateau segment. All discussed ^{39}Ar-^{40}Ar results are displayed at the 2σ level.

5.2. Results

All analyses, except one, allowed plateau age calculations (Fig. 6; Table 2). The two whole rock fragments from sample BEK2 displayed concordant plateau ages with a mean age at 13.9 ± 0.2 Ma.

Biotite from sample BEK11 showed a flat age spectrum with a significant plateau age at 14.4 ± 0.2 Ma (98.5% of total $^{39}Ar_K$ degassed). In contrast the corresponding whole rock fragment yielded a slightly hump-shaped age spectrum which did not allow plateau age definition. This shape and the integrated age at 15.6 ± 0.2 Ma, slightly higher than biotite age, could suggest sample disturbance related to $^{39}Ar_K$ recoil during irradiation.

The biotite age spectrum from sample BEK22 showed a flat pattern with a calculated plateau age at 14.6 ± 0.2 Ma (98.6% of total $^{39}Ar_K$ degassed). The corresponding whole

Table 2: $^{40}Ar/^{39}Ar$ analytical data. $^{40}Ar_{atm}$ = atmospheric ^{40}Ar. $^{40}Ar^{*}$ = radiogenic ^{40}Ar. Ca= produced by Ca-neutron interferences. K= produced by K-neutron interferences. Age (Ma)= the date is calculated using the decay constants recommended by Steiger & Jäger [116]. The errors are at the 1σ level and do not include the error in the value of the J parameter. Correction factors for interfering isotopes produced by neutron irradiation in the McMaster reactor were $(^{39}Ar/^{37}Ar)_{Ca} = 7.06\times10^{-4}$, $(^{36}Ar/^{37}Ar)_{Ca} = 2.79\times10^{-4}$, $(^{40}Ar/^{39}Ar)_{K} = 2.97\times10^{-2}$.

Step	$^{40}Ar_{Atm.}$(%)	$^{39}Ar_{K.}$(%)	$^{37}Ar_{Ca}/^{39}Ar_{K}$	$^{40}Ar^{*}/^{39}Ar_{K}$	Age (Ma)		
BEK2 Whole Rock			J= 0.00036699				
1	99.1	1.0	1.19	3.37	52.9	±	33.4
2	98.9	0.2	2.09	0.79	12.5	±	15.3
3	96.2	1.3	2.57	0.89	14.1	±	3.0
4	88.5	4.8	2.47	0.80	12.7	±	0.9
5	54.3	6.9	1.63	0.98	15.5	±	0.3
6	28.1	11.0	1.61	0.93	14.7	±	0.2
7	18.4	13.5	1.75	0.91	14.5	±	0.2
8	12.7	8.2	1.67	0.88	14.0	±	0.4
9	8.4	7.3	1.87	0.88	14.0	±	0.4
10	8.0	9.0	2.17	0.87	13.9	±	0.2
11	5.4	11.9	1.78	0.88	13.9	±	0.2
12	8.2	9.8	2.05	0.87	13.8	±	0.3
Fusion	19.0	15.2	3.24	0.86	13.7	±	0.3
				Integrated age	14.5	±	0.3
BEK2 Whole Rock			J= 0.00036699				
1	99.7	1.1	1.25	1.00	15.9	±	32.0
2	96.1	0.6	2.74	0.96	15.2	±	10.7
3	99.3	1.1	2.53	0.05	0.8	±	3.6
4	81.6	5.0	2.39	0.85	13.6	±	1.7
5	38.9	4.3	1.30	0.92	14.6	±	1.5
6	21.2	12.5	1.65	0.93	14.7	±	0.4
7	17.7	12.0	1.75	0.86	13.7	±	0.4
8	15.0	10.8	1.54	0.81	12.8	±	0.5
9	11.3	7.6	1.83	0.82	13.1	±	0.6
10	11.1	7.8	2.08	0.82	13.0	±	0.9
11	8.5	14.2	1.49	0.84	13.3	±	0.3
12	9.8	10.1	1.78	0.85	13.5	±	0.4
Fusion	12.0	12.8	3.77	0.87	13.8	±	0.4
				Integrated age	13.5	±	0.4
BEK11 Biotite			J= 0.00036703				
1	93.6	0.3	0.00	0.47	7.5	±	7.4
2	100.0	0.1	0.00	0	0.0	±	0.0
3	80.6	0.5	0.13	0.44	6.9	±	4.2
4	76.7	0.5	0.03	0.42	6.7	±	4.1
5	57.1	1.3	0.13	0.86	13.6	±	1.6
6	25.8	3.1	0.06	0.90	14.3	±	0.7
7	19.2	5.2	0.04	0.88	13.9	±	0.4
8	11.3	8.8	0.02	0.92	14.7	±	0.3
9	10.6	9.7	0.02	0.91	14.5	±	0.3
10	9.9	11.1	0.03	0.91	14.5	±	0.2
11	10.7	14.0	0.04	0.90	14.3	±	0.1
12	7.6	11.3	0.03	0.91	14.5	±	0.2
13	6.3	18.0	0.02	0.91	14.4	±	0.1
14	5.8	7.1	0.01	0.90	14.2	±	0.3
Fusion	6.0	9.1	0.01	0.91	14.4	±	0.2
				Integrated age	14.3	±	0.1

BEK11 Whole Rock			J= 0.00036714				
1	78.1	13.0	0.21	0.99	15.7	±	0.4
2	71.0	10.1	0.21	0.93	14.8	±	0.4
3	62.4	14.2	0.27	1.00	15.9	±	0.2
4	51.7	14.8	0.37	1.04	16.5	±	0.2
5	44.4	13.8	0.67	1.00	15.8	±	0.2
6	40.2	12.5	1.42	0.95	15.1	±	0.2
7	30.6	8.4	1.92	0.92	14.6	±	0.2
8	35.4	6.8	2.27	0.88	14.0	±	0.2
9	40.6	3.0	2.77	0.88	13.9	±	0.4
10	40.3	1.0	3.75	0.91	14.5	±	0.6
11	47.4	2.3	5.85	1.40	22.2	±	0.7
				Integrated age	15.6	±	0.1
BEK22 biotite			J= 0.00036718				
1	95.3	0.2	0.99	0.98	15.6	±	11.7
2	89.1	0.1	1.67	0.52	8.2	±	14.7
3	64.8	0.5	1.51	0.79	12.6	±	5.0
4	66.4	0.6	1.46	0.66	10.4	±	4.7
5	46.4	2.4	0.50	0.92	14.7	±	1.1
6	14.7	4.1	0.07	0.97	15.4	±	0.6
7	10.8	7.2	0.04	0.94	14.9	±	0.3
8	10.8	8.7	0.04	0.91	14.4	±	0.3
9	10.5	13.4	0.05	0.91	14.5	±	0.2
10	8.0	19.9	0.03	0.91	14.4	±	0.2
11	4.6	16.9	0.03	0.93	14.7	±	0.2
12	4.1	10.8	0.02	0.93	14.7	±	0.2
13	6.0	11.5	0.02	0.91	14.5	±	0.3
Fusion	7.5	3.9	0.02	0.91	14.5	±	0.7
				Integrated age	14.6	±	0.1
BEK22 Whole Rock			J=0,00036722				
1	96.5	0.5	0.81	2.09	33.1	±	8.2
2	93.1	0.7	0.78	1.74	27.5	±	4.3
3	85.0	2.5	0.34	1.26	20.0	±	1.4
4	39.5	8.9	0.30	1.02	16.1	±	0.3
5	15.2	5.5	0.27	1.00	15.9	±	0.3
6	17.3	8.5	0.30	0.96	15.3	±	0.2
7	13.9	7.1	0.28	0.93	14.8	±	0.3
8	12.9	7.1	0.31	0.92	14.7	±	0.2
9	13.4	9.1	0.35	0.92	14.6	±	0.2
10	13.3	6.5	0.38	0.90	14.3	±	0.2
11	11.1	8.4	0.45	0.93	14.8	±	0.2
12	12.6	6.9	0.53	0.90	14.3	±	0.2
13	10.9	7.6	0.66	0.91	14.5	±	0.2
14	12.1	5.7	0.83	0.90	14.3	±	0.2
15	9.6	6.5	1.03	0.93	14.7	±	0.2
16	12.7	4.5	1.57	0.90	14.3	±	0.3
17	15.8	1.4	2.16	0.92	14.6	±	0.9
18	27.1	2.5	4.55	0.94	14.9	±	0.8
				Integrated age	15.2	±	0.1

rock showed an age spectrum with decreasing apparent ages in the low temperature steps, probably related to a small $^{39}Ar_K$ recoil effect, and a flat pattern in the intermediate to high temperature steps (73.4% of total $^{39}Ar_K$ degassed), allowing a plateau age calculation at 14.6 ± 0.1 Ma, highly concordant with corresponding biotite result.

6. Comparison with Other Tertiary Intermediate Magmatic Suites in Western Turkey

As the magmatism associated with the Küçük Menderes Graben is perceived as related to general extensional tectonics in Western Anatolia, a comparison was made with other contemporaneous and penecontemporaneous volcanic rocks in the area. When K_2O, Ba and Sr are plotted against SiO_2 (Fig. 7a–c), a comparison with intermediate volcanic rocks from the Biga Peninsula [80] shows that the latter are richer in all three of these elements than the Küçük Menderes volcanics. By contrast, a TiO_2-V diagram (Fig. 7d) shows that whereas the Küçük Menderes volcanics form a compact fractionation trend of V depletion with little change in TiO_2 content, the generally more TiO_2-depleted volcanic rocks from the Biga Peninsula fall on a separate trend of proportionately declining V and TiO_2. Comparison with other magmatic suites studied by Erkül *et al.* [13] tends to show even less comparability (Fig. 8a, b). Most of the magmatic rocks studied by Innocenti *et al.* [60] and Seyitoğlu *et al.* [74] comprise ultrapotassic suites including shoshonites and lamproites, which are utterly unlike the Küçük Menderes volcanic rocks (Fig. 8c–e). However, the calc-alkaline suite studied by Innocenti *et al.* [60] has comparable K_2O to the Biga Peninsula suites studied by Aldanmaz *et al.* [80].

It is difficult to be certain why the Küçük Menderes volcanic rocks are chemically so different from penecontemporaneous volcanic rocks to the north of the Gediz Graben. An explanation citing basement control does not seem initially to be readily applicable, as the core Menderes Massif rocks underlie both areas.

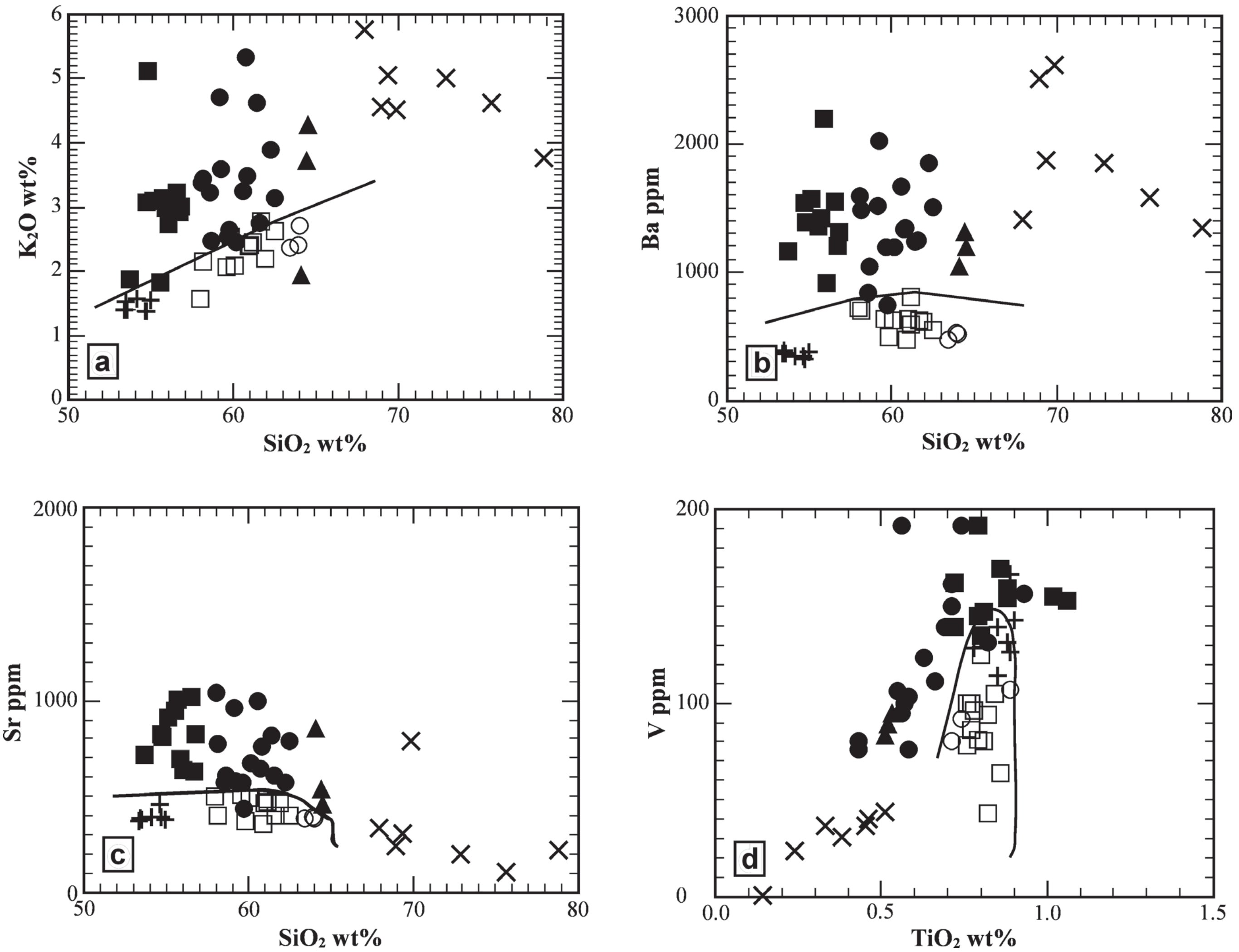

Fig. 7: Comparision of Kiraz volcanics with intermediate volcanic rocks from the Biga Peninsula [80]. **(a)** K_2O *vs* SiO_2; **(b)** Ba *vs* SiO_2, **(c)** Sr *vs* SiO_2 and **(d)** TiO_2 *vs* SiO_2 diagrams. Kiraz Volcanics (this study). Symbols: upright crosses– Yenişehir basaltic andesite, open squares– Karaburç andesite, open circle– Bozdağ dacite; Biga volcanics [80]: filled squares– basalts/trachyandesites, filled circles– trachyandesites, filled upright triangles– dacites, diagonal crosses– rhyolites.

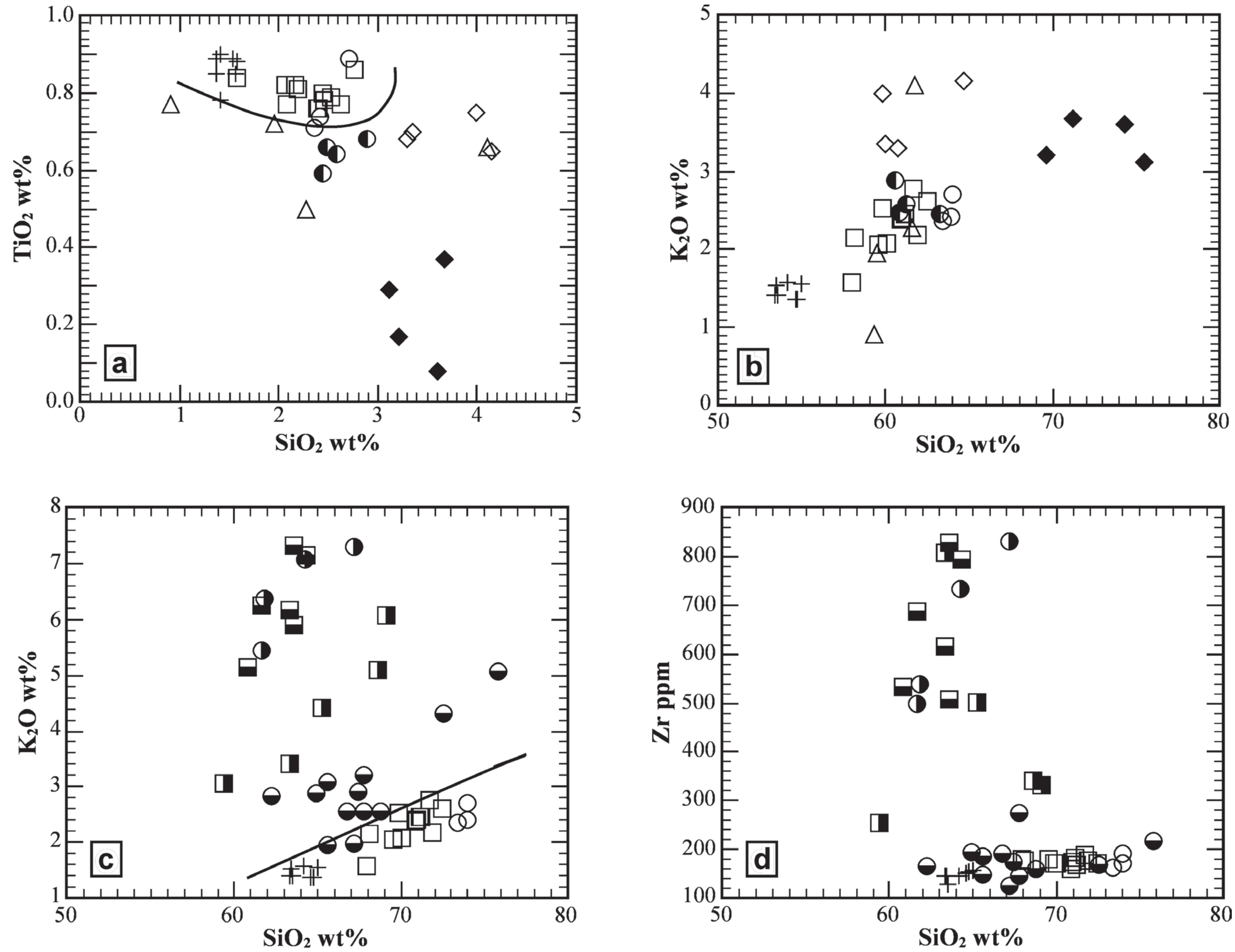

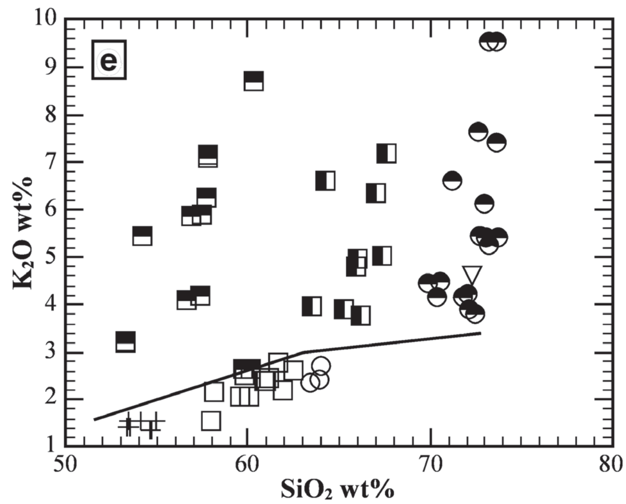

Fig. 8: Comparision of Kiraz volcanics with other volcanic rocks of western Anatolia. **(a)** TiO_2 *vs* SiO_2 and **(b)** K_2O *vs* SiO_2 diagrams showing comparison with Bigadiç volcanics [13]. Symbols: Open upright triangles– Kocaiskan age? volcanics (ca. 23 Ma), filled diamonds– Sındırgı volcanics (ca. 19-20 Ma), open diamonds– Kayırlar volcanics (ca. 20 Ma), half-filled circles, shaded to left– Şahinkaya volcanics (ca. 18 Ma). **(c)** K_2O *vs* SiO_2 and **(d)** Zr *vs* SiO_2 diagrams, showing comparison with Neogene–Quaternary volcanics studied by Innocenti *et al*. (2007). Symbols: Half-filled circle, shaded below– calc-alkaline rocks, half-filled squares, shaded to right– shoshonites rocks, half-filled squares, shaded below– ultrapotassic rocks, half-filled circles, shaded to right– lamproites. **(e)** K_2O *vs* SiO_2 diagram showing comparison with Miocene–Quaternary volcanics studied by Seyitoğlu *et al*. (1997). Symbols: Half-filled circles, shaded above– rhyolites, half-filled squares, shaded to left– dacites, half-filled squares, shaded above– andesites. Kiraz Volcanics (this study): upright crosses– Yenişehir basaltic andesite, open squares– Karaburç andesite, open circle– Bozdağ dacite.

However, tectonic maps of Western Anatolia showing the recent extensional faulting pattern also reveal that there is a marked change of orientation between areas north and south of the Gediz Graben, suggesting that perhaps there is indeed some basement control. An examination of the distribution of enclaves within the core Menderes orthogneisses reveals the presence of eclogitic remnants southwest of the Gediz Graben: no such remnants have been recorded to the northeast, and this may suggest that the Gediz Graben could mark the reactivation of a basement lineament separating different pre-orthogneiss basement types.

7. Discussion and Conclusions

Miocene volcanic rocks from the Küçük Menderes graben cover such small areas that they might easily be overlooked. However, although their potassium contents are higher than that of evolved tholeiitic rocks, they appear to form one of the least potassic suites of Tertiary calc-alkaline volcanic rocks in Western Anatolia, and hence are important indicators of the palaeotectonic environment. By contrast, the potassic magmatism to the northeast is similar to that seen elsewhere in the Mediterranean area [113], such as the Roman Province of Italy, and the higher K_2O content of these rocks is generally interpreted as the result of derivation from enriched mantle sources, tapped during the aftermath of a continental collisional event. Across northwestern Anatolia the potassium content of the magmatic suites tends to be higher to the north, and this could reflect changing magmatic source rocks at depth, relating to greater proximity to the point of Miocene continental convergence. Equally, however, differences of age of emplacement, at a time of rapidly changing tectonic environment, with progressive southwestward migration of the subduction hinge, might also be the cause.

North of the Gediz Graben, the Miocene continental collision, and subsequent extension, were the last major regional tectonic events to have occurred. Further south, however, graben development becomes an increasingly dominant feature of late Tertiary tectonics, while the southwest of Anatolia impinges on the eastern end of the Southern Aegean Arc, which extends across the southern Aegean Sea (Fig. 1). We believe that the chemistry of the volcanic rocks from the Kiraz basin reflects both their relative youth at a time of rapidly-changing tectonic settings, their association with regional NW–SE trending faulting, and their proximity to the Southern Aegean Arc. The chemical contribution from the northward-descending slab accounts for the calc-alkaline chemistry of the lavas, even though they were erupted in grabens. Hence contamination of the magma, emplaced in an extensional setting (which would normally be characterized by tholeiitic magmas), produced the calc-alkaline composition of the Kiraz Basin magmatic suites.

Acknowledgements

This work was founded by TÜBİTAK grant 104Y154 and METU Research Foundation grant BAP–2004-03-09-03. Analytical assistance was provided by D.W. Emley and M. Aikin at Keele University. The authors are thankful to Samuele Agostini for his comments that improved an early version of the present text.

References

[1] A.M.C. Şengör, Y. Yılmaz, Tethyan evolution of Turkey: a plate tectonic approach, Tectonophysics 75 (1981) 181–241.

[2] A.M.C. Şengör, N. Görür, F. Şaroğlu, Strike-slip faulting and related basin formation in zones of tectonic escape: Turkey as a case study, in: K. Biddle, N. Christie-Blick, (Eds), Strike-Slip Deformation, Basin Formation and Sedimentation. Soc. Econ. Paleont. Miner., Spec. Publ. 37, 1985, pp. 227–64.

[3] E. Bozkurt, Neotectonics of Turkey – a synthesis, Geodinamica Acta 14 (2001) 3–30.

[4] E. Bozkurt, S.K. Mittwede, Introduction: Evolution of Neogene extensional tectonics of western Turkey, Geodinam. Acta 18 (2005) 153–165.

[5] Ç. Özkaymak, H. Sözbilir, Stratigraphic and structural evidence for fault reactivation: the active Manisa fault zone, Western Anatolia, Turkish J. Earth Sci. 17 (2008) 615–635.

[6] E. Arpat, E. Bingöl, The rift system in western Turkey: through on its developments, MTA Bull. 79 (1969), 1–9 [in Turkish with English Abstract].

[7] H. Eyidoğan, J.A. Jackson, A seismological study of normal faulting in the Demirci, Alaşehir and Gediz earthquake of 1960–1970 in western Turkey: implications for the nature and geometry of deformation in the continental crust, Geophys. Jour. Royal Astron. Soc. 81 (1985) 569–607.

[8] E. Firuzan, Statistical earthquake frequency analysis for western Anatolia, Turkish J. Earth Sci. 17 (2008) 741–762.

[9] O. Pamukçu, A. Yurdakul, Isostatic compensation in Western Anatolia with estimate of the effective elastic thickness, Turkish J. Earth Sci. 17 (2008) 545–557.

[10] O. Polat, E. Gök, Y. Doğruer, Earthquake Hazard of the Aegean Extension Region (W. Turkey), Turkish J. Earth Sci. 17 (2008) 593–614.

[11] O.M. Tan, C. Tapırdamaz, A. Yörük, The earthquake catalogues for Turkey, Turkish J. Earth Sci. 17 (2008) 405–418.

[12] F. Erkül, H. Helvacı, H. Sözbilir, Stratigraphy and geochronology of the Early Miocene volcanic units in the Bigadiç borate basin, Western Turkey, Turkish J. Earth Sci. 14 (2005) 227–253.

[13] F. Erkül, H. Helvacı, H. Sözbilir, Evidence for two episodes of volcanism in the Bigadic borate basin and tectonic implications for western Turkey, Geol. Jour. 40 (2005) 545–570.

[14] M. Tokcaer, S. Agostini, M.Y. Savaşçın, Geotectonic setting and origin of the youngest Kula volcanics (Western Anatolia), with a new emplacement model, Turkish J. Earth Sci. 14 (2005) 143–166.

[15] E. Aldanmaz, Mineral-chemical constraints on the Miocene calc-alkaline and shoshonitic volcanic rocks of Western Turkey: disequilibrium phenocryst assemblages as indicators of magma storage and mixing conditions, Turkish J. Earth Sci. 15 (2006) 47–73.

[16] Y. Ersoy, C. Helvacı, Stratigraphy and geochemical features of the Early Miocene bimodal (ultrapotassic and calc-alkaline) volcanic activity within the NE-trending Selendi Basin, Western Anatolia, Turkey, Turkish J. Earth Sci. 16 (2007) 117–139.

[17] Z. Karacık, Y. Yılmaz, J.A. Pearce, The Dikili-Çandarlı volcanics, Western Turkey: magmatic interactions as recorded by petrographic and geochemical features, Turkish J. Earth Sci. 16 (2007) 493–522.

[18] Y. Ersoy, C. Helvacı, H. Sözbilir, F. Erkül, E. Bozkurt A geochemical approach to Neogene–Quaternary volcanic activity of western Anatolia: an example of episodic bimodal volcanism within the Selendi Basin, Turkey, Chem. Geol. 255 (2008) 265–282.

[19] Y. Yücel-Öztürk, C. Helvacı, M. Satır, Genetic relations between skarn mineralization and petrogenesis of the Evciler Granitoid, Kazdağ, Çanakkale, Turkey and comparison with world skarn granitoids, Turkish J. Earth Sci. 14 (2005) 225–280.

[20] A. Sayın, Origin of kaolin deposits: evidence from the Hisarcık (Emet-Kütahya) deposits, western Turkey, Turkish J. Earth Sci. 16 (2007) 77–96.

[21] H. Yılmaz, Stream sediment geochemical exploration for gold in the Kazdağ dome in the Biga Peninsula, western Turkey, Turkish J. Earth Sci. 16 (2007) 33–55.

[22] H. Mutlu, Constraints on the origin of the Balıkesir thermal waters (Turkey) from stable isotope ($\delta^{18}O$, δD, $\delta^{13}C$, $\delta^{34}S$) and major-trace element compositions, Turkish J. Earth Sci. 16 (2007) 13–32.

[23] J.E. Meulenkamp, W.J.R. Wortel, W.A. Van Wamel, W. Spakman, E. Hoogerduyn Strating, On the Hellenic subduction zone and geodynamic evolution of Crete in the late Middle Miocene, Tectonophysics 146 (1988) 203–215.

[24] J.E. Meulenkamp, G.J. Van Der Zwaan, W.A. Van Wamel, On Late Miocene to recent vertical motions in the Cretan segment of the Hellenic arc, Tectonophysics 234 (1994) 53–72.

[25] C. Kissel, C. Laj, Tertiary geodynamical evolution of the Aegean arc: a palaeomagnetic reconstruction, Tectonophysics 146 (1988) 183–201.

[26] S.N. Thomson, B. Stöckhert, M.R. Brix, Thermochronology of the high-pressure metamorphic rocks of Crete, Greece: implications for the speed of tectonic processes, Geology 26 (1998) 259–262.

[27] J.F. Dewey, A.M.C. Şengör, Aegean and surrounding region: Complex multiplate and continuum tectonics in a convergent zone, *Geol. Soc. Amer. Bull.* 90 (1979) 84–92.

[28] A.M.C. Şengör, Cross-faults and differential stretching of hanging walls in regions of low-angle normal faulting: examples from eastern Turkey. in: M.P. Coward, J.F. Dewey, P.L. Hancock, (Eds), Continental Extensional Tectonics. Geol. Soc. London, Spec. Publ. 28, 1987, pp. 575–589.

[29] J.F. Dewey, Extensional collapse of orogens. Tectonics 7 (1988) 1123–1139.

[30] G. Seyitoğlu, B.C. Scott, Late Cenozoic crustal extension and basin formation in west Turkey, Geol. Mag. 28 (1991) 155–166.

[31] G. Seyitoğlu, B. Scott, The age of the Büyük Menderes Graben (west Turkey) and its tectonic implications, Geol. Mag. 129 (1992) 239–242.

[32] C. Doglioni, S. Agostini, M. Crespi, F. Innocenti, P. Manetti, F. Riguzzi, M.Y. Savaşçın, On the extension in western Anatolia and the Aegean Sea, Virtual Explorer 8 (2002) 169–183.

[33] G. Seyitoğlu, İ. Çemen, O. Tekeli, Extensional folding in the Alaşehir Gediz graben, western Turkey, J. Geol. Soc. London 157 (2000) 1097–1100.

[34] G. Seyitoğlu, V. Işık, İ. Çemen, Complete Tertiary exhumation history of the Menderes Massif, western Turkey: an alternative working hypothesis. Terra Nova 16 (2004) 358–363.

[35] G. Seyitoğlu, O. Tekeli, İ. Çemen, Ş. Şen, V. Işık, The role of flexural rotation/rolling hinge model in the tectonic evolution of the Alaşehir graben, western Turkey, Geol. Mag. 139 (2002) 15–26.

[36] J. Glodny, R. Hetzel, Prices U-Pb ages of syn-extensional Miocene intrusions in the central Menderes Massif, western Turkey, Geol. Mag. 144 (2007) 235–246.

[37] A. Koçyiğit, H. Yusufoğlu, E. Bozkurt, Evidence from the Gediz graben for episodic two-stage extension in western Turkey, J. Geol. Soc. London, 156 (1999) 605–616.

[38] Y. Yılmaz, S.C. Genç, Ö.F. Gürer, M. Bozcu, K. Yılmaz, Z. Karacık, Ş. Altunkaynak, A. Elmas, When did western Anatolian grabens begin to develop, in: E. Bozkurt, J.A. Winchester, J.D.A. Piper (Eds), Tectonics and Magmatism in Turkey and the Surrounding Area. Geol. Soc. London, Spec. Publ. 173, 2000, pp. 353–384.

[39] E. Bozkurt, 2001, Late Alpine evolution of central Menderes Massif, western Anatolia, Turkey, Inter. J. Earth Sci. 89, 728–744.

[40] E. Bozkurt, H. Sözbilir, Tectonic evolution of the Gediz Graben: field evidence for an episodic, two-stage extension in western Turkey, Geol. Mag. 141 (2004) 63–79.

[41] E. Bozkurt, H. Sözbilir, Evolution of the large-scale Active Manisa Fault, Southwest Turkey: implications on fault development and regional tectonics, Geodinam. Acta 19 (2006) 427–453.

[42] O. Kaya, E. Ünay, F. Göktaş, G. Saraç, Early Miocene stratigraphy of Central West Anatolia, Turkey: implications for the tectonic evolution of the Eastern Aegean area, Geol. Jour. 49 (2007) 85–109.

[43] O. Kaya, E. Ünay, G. Saraç, S. Eichhorn, S. Hassenrück, A. Knappe, A. Pekdeğer, S. Mayda, Halitpaşa transpressive zone: implications for an Early Pliocene compressional phase in central western Anatolia, Turkey, Turkish J. Earth Sci. 13 (2004) 1–13.

[44] M. Purvis, A.H.F. Robertson, Miocene sedimentary evolution of the NE–SW-trending Selendi and Gördes basins, W Turkey: implications for extensional processes, Sed. Geol. 174 (2005) 31–62.

[45] M. Purvis, A.H.F. Robertson, M. Pringle Ar^{40}-Ar^{39} dating of biotite and sanidine in tuffaceous sediments and related intrusive rocks: Implications for the Early Miocene evolution of the Gördes and Selendi basins, W Turkey, Geodinam Acta 18 (2005) 239–253.

[46] L. Beccaletto, C. Steiner, Evidence of two-stage extensional tectonics from the northern edge of the Edremit Graben, NW Turkey, Geodinam. Acta 18 (2005) 283–297.

[47] E. Bozkurt, B. Rojay, Episodic, two-stage Neogene extension and short-term intervening compression in western Anatolia: field evidence from the Kiraz basin and Bozdağ horst, Geodinam. Acta 18 (2005) 299–316.

[48] N. Kaymakcı, Kinematic development and paleostress analysis of the Denizli Basin (Western Turkey): implications of spatial variation of relative paleostress magnitudes and orientations, J. Asian Earth Sci. 27 (2005) 207–222.

[49] A. Koçyiğit, The Denizli graben-horst system and the eastern limit of western Anatolian continental extension: basin fill, structure, deformational mode, throw amount and episodic evolutionary history, Geodinam. Acta 18 (2005) 167–208.

[50] T. Emre, H. Sözbilir, Tectonic evolution of the Kiraz Basin, Küçük Menderes Graben: evidence for compression/uplift-related basin formation overprinted by extensional tectonics in West Anatolia, Turkish J. Earth Sci. 16 (2007) 441–470.

[51] A. Koçyiğit, Ş. Deveci, A N–S-trending active extensional structure, the Şuhut (Afyon) graben: commencement age of the extensional neotectonic period in the Isparta Angle, SW Turkey, Turkish J. Earth Sci. 16 (2007) 391–416.

[52] E. Özsayın, K. Dirik, Quaternary activity of the Cihanbeyli and Yeniceoba Fault zones: İnonu-Eskişehir Fault System, Central Anatolia, Turkish J. Earth Sci. 16 (2007) 471–492.

[53] B. Rojay, V. Toprak, C. Demirci, L. Süzen, Plio–Quaternary evolution of the Küçük Menderes Graben Southwestern Anatolia, Turkey, Geodinam. Acta 18 (2005) 317–331.

[54] N.B. Çiftçi, E. Bozkurt, Anomalous stress field and active breaching in relay ramps: A field example from Gediz Graben, SW Turkey, Geol. Mag. 144 (2007) 687–699.

[55] N.B. Çiftçi, E. Bozkurt, Pattern of normal faulting in the Gediz Graben, SW Turkey, Tectonophysics, (2008) doi:10.1016/j.tecto.2008.05.036 [in press].

[56] N.B. Çiftçi, E. Bozkurt, Folding of the Gediz Graben fill, SW Turkey: extensional and/or contractional origin?, Geodinam. Acta 21 (2008) 145–167.

[57] B. Uzel, H. Sözbilir, A First record of strike-slip basin in western Anatolia and its tectonic implication: The Cumaovası basin as an example, Turkish J. Earth Sci. 17 (2008) 559–591.

[58] G. Seyitoğlu, B.C. Scott, Late Cenozoic basin development in western Turkey: Gördes Basin: tectonics and sedimentation, Geol. Mag. 131 (1994) 631–637.

[59] G. Seyitoğlu, Late Cenozoic tectono-sedimentary development of the Selendi and Uşak-Güre basins: a contribution to the discussion on the development of east–west and north trending basins in western Turkey, Geol. Mag. 134 (1997) 163–175.

[60] F. Innocenti, D. Agostini, G. Di Vincenzo, C. Doglioni, P. Manetti, M.Y. Savaşçın, S. Tonarini Neogene and Quaternary volcanism in Western Anatolia: magma sources and geodynamic evolution, Marine Geol. 221 (2005)397–421.

[61] S. Altunkaynak, Y. Dilek, Timing and nature of postcollisional volcanism in western Anatolia and geodynamic implications, in: Y. Dilek, S. Pavlides (Eds), Postcollisional Tectonics and Magmatism in the Mediterranean Region and Asia. Geol. Soc. America Spec. Paper 409, 2006, pp. 321–351.

[62] L. Beccaletto, N. Bonev, D. Bosch, O. Bruguier, Record of a Palaeogene syn-collisional extension in the north Aegean region: evidence from the Kemer micaschists (NW Turkey), Geol. Mag. 144 (2007)393–400.

[63] Y. Dilek, Ş. Altunkaynak, Cenozoic crustal evolution and mantle dynamics of post-collisional magmatism in western Anatolia, Inter. Geol. Rev. 49 (2007) 431–453.

[64] J. Borsi, G. Ferrara, F. Innocenti, R. Mazzuoli, Geochronology and petrology of recent volcanics in the eastern Aegean sea (western Anatolia and Lesvos island), Bull. Volcanology 36 (1972) 473–496.

[65] E. Bingöl, M. Delaloye, G. Ataman, Granitic intrusions in western Anatolia: a contribution to the geodynamic evolution of this area, Eclog. Geol. Helvet. 75 (1982) 437–446.

[66] T. Ercan, Batı Anadolunun genç tektoniği ve volkanizması. *TJK Batı Anadolunun Genç Tektoniği ve Volkanizması Paneli*, 1982, 5–14.

[67] M. Fytikas, F. Innocenti, P. Manetti, R. Mazzuoli, A. Peccerillo, L. Villari Tertiary to Quaternary evolution of the volcanism in the Aegean region. in: J.E. Dixon, A.H.F. Robertson, (Eds), The Geological Evolution of the Eastern Mediterranean. Geol. Soc. London, Spec. Publ. 17, 1984, pp. 687–700.

[68] T. Ercan, M. Satır, H. Kreuzer, A. Türkecan, E. Günay, A. Çevkikbaş, M. Ateş, B. Can, Batı Anadolu Senozoyik volkaniklerine ait yeni kimyasal, izotopik ve radyometrik verilerin yorumu, Geol. Soc. Bull., Turkey 28 (1985) 121–136 [in Turkish with an English abstract].

[69] T. Ercan, M. Satır, G. Steinitz, A. Dora, E. Sarıfakıoğlu, C. Adis, H.J. Walter, T. Yıldırım, Biga yarımadası ile Gökçeada, Bozcaada ve Tavşan adalarındaki (KB Anadolu) Tersiyer volkanizmasının özellikleri, MTA Bull. 117 (1995) 55–86 [in Turkish with an English abstract].

[70] T. Ercan, M. Satır, D. Sevin, A.Türkecan, Batı Anadolu’daki Tersiyer ve Kuvarterner yaşlı kayaçlarda yeni yapılan radyometrik yaş ölçümlerinin yorumu, MTA Bull. 119 (1997) 103–112 [in Turkish with an English abstract].

[71] Y. Yılmaz, An approach to the origin of young volcanic rocks of western Turkey. in: A.M.C. Şengör, (Ed), Tectonic Evolution of Tethyan Region. Nato ASI. Kluwer, The Hague 259, 1989, pp. 159–189.

[72] Y. Yılmaz, Comparison of young volcanic associations of western and eastern Anatolia under compressional regime: a review. J. Volcan. Geother. Res. 44 (1990) 69–87.

[73] N. Güleç, Crust-mantle interaction in western Turkey: implications from Sr and Nd isotope geochemistry of Tertiary and Quaternary volcanics, Geol. Mag. 123 (1991) 417–435.

[74] G. Seyitoğlu, D. Anderson, G. Nowell, B. Scott, The evolution from Miocene potassic to Quaternary sodic magmatism in western Turkey: implications for enrichment processes in the lithospheric mantle, J. Volcan. Geother. Res. 76 (1997) 127–147.

[75] E. Aydar, Early Miocene to Quaternary evolution of volcanism and the basin formation in western Anatolia: a review, J. Volcan. Geother. Res. 85 (1998) 69–82.

[76] Ş. Altunkaynak, Y. Yılmaz, The Kozak magmatic complex, western Anatolia, J. Volcan. Geother. Res. 85 (1998) 211–231.

[77] Ş. Altunkaynak, Y. Yılmaz, The Kozak pluton and its emplacement, Geol. Jour. 34 (1999) 257–274.

[78] Ş.C. Genç, Evolution of Bayramiç magmatic omplex, J. Volcan. Geother. Res. 85 (1998) 233–249.

[79] Z. Karacık, Y. Yılmaz, Geology of the ignimbrites and the associated volcano-plutonic complex of the Ezine area, northwestern Anatolia, J. Volcan. Geother. Res. 85 (1998) 251–264.

[80] E. Aldanmaz, J.A. Pearce, M.F. Thirlwall, J.G. Mitchell, Petrogenetic evolution of late Cenozoic, post-collision volcanism in western Anatolia, Turkey, J. Volcan. Geother. Res. 102 (2000) 67–95.

[81] M. Delaloye, E. Bingöl, Granitoids from western and northwestern Anatolia: geochemistry and modeling of geodynamic evolution, Inter. Geol. Rev. 42 (2000) 241–268.

[82] Y. Yılmaz, Ş.C. Genç, Z. Karacık, Ş. Altunkaynak, Two constrasting magmatic associations of NW Anatolia and their tectonic significance, Jour. Geodynamics 31 (2001) 243–271.

[83] E. Aldanmaz, Mantle source characteristics of alkalin basalts and basanites in an extensional intracontinental plate setting, western Anatolia, Turkey: implications for multi-stage melting, Inter. Geol. Rev. 44 (2002) 440–457.

[84] R. Hetzel, U. Ring, C. Akal, M. Troesch, Miocene NNE-directed extensional unroofing in the Menderes Massif, southwestern Turkey, J. Geol. Soc. London 152 (1995) 639–654.

[85] V. Işık, O. Tekeli, Late orogenic crustal extension in the northern Menderes Massif (western Turkey): evidence for metamorphic core complex formation, Inter. J. Earth Sci. 89 (2001) 757–765.

[86] V. Işık, O. Tekeli, G. Seyitoglu, Ductile-brittle transition along the Alaşehir detachment fault and its structural relationship with the Simav detachment fault, Menderes Massif, western Turkey, Tectonophysics 374 (2003) 1–18.

[87] E. Bozkurt, Granitoid rocks of the southern Menderes Massif (southwest Turkey): field evidence for Tertiary magmatism in an extensional shear zone, Inter. J. Earth Sci. 93 (2004) 52–71.

[88] U. Ring, A.S. Collins, U-Pb SIMS dating of syn-kinematic granites: timing of core-complex formation in the northern Anatolide belt of western Turkey, J. Geol. Soc. London 162 (2005) 289–298.

[89] S. Agostini, C. Doglioni, F. Innocenti, P. Manetti, S. Tonarini, S., M.Y. Savaşçın, The transition from subduction-related to intraplate Neogene magmatism in the Western Anatolia and Aegean area. in: L. Beccaluva, G. Bianchini, M. Wilson, (Eds), Cenozoic Volcanism in the Mediterranean Area. Geol. Soc. America Spec. Paper 418, 2007, pp. 1–15.

[90] R. Westaway, H. Guillou, S. Yurmen, T. Demir, G. Rowbotham, Constraints on the timing and regional conditions at the start of the present phase of extension in western Turkey, from observations in and around the Denizli region, Geodinam. Acta 18 (2005) 209–238.

[91] R. Westaway, M. Pringle, S. Yurtmen, T. Demir, D. Bridgland, G. Rowbotham, D. Maddy, Pliocene and Quaternary regional uplift in western Turkey: the Gediz River terrace staircase and the volcanism at Kula, Tectonophysics 391 (2004) 121–169.

[92] S. Tonarini, S. Agostini, F. Onnocenti, P. Manetti, δ^{11} B as tracer of slab dehydration and mantle evolution in western Anatolia Cenozoic magmatism, Terra Nova 17 (2005) 259–264.

[93] E. Aldanmaz, N. Köprübaşı, Ö.F. Gürer, N. Kaymakcı, A. Gourgaud, Geochemical constraints on the Cenozoic, OIB-type alkaline volcanic rocks of NW Turkey: Implications for mantle sources and melting processes, Lithos 86 (2006) 50–76.

[94] S. Altunkaynak, Collision-driven slab breakoff magmatism in northwestern Anatolia, Turkey, J. Geol. 115 (2007) 63–82.

[95] N. Kaymakcı, E. Aldanmaz, C. Langereis, T.L. Spell, O.F. Gürer, K.A. Zanetti, Late Miocene transcurrent tectonics in NW Turkey: evidence from palaeomagnetism and ^{40}Ar-^{39}Ar dating of alkaline volcanic rocks, Geol. Mag. 144 (2007) 379–392.

[96] H. Yılmaz, M. Alpaslan, A. Temel, Two-stage felsic volcanism in the western part of the southeastern Anatolian orogen: petrologic and geodynamic implications, Inter. Geol. Rev. 49 (2007) 120–141.

[97] J.M. Richardson-Bunbury, The Kula volcanic field, western Turkey: the development of a Holocene alkali basal province and the adjacent normal faulting, Geol. Mag. 133 (1996) 275–283.

[98] J.M. Bunbury, L. Hall, G.J. Anderson, A. Stannard, The determination of fault movement history from the interaction of local drainage with volcanic episodes, Geol. Mag. 138 (2001)185–192.

[99] P. Alıcı, A. Temel, A. Gourgaud, Pb-Nd-Sr isotope and trace element geochemistry of Quaternary extension-related alkaline volcanism: a case study of Kula region (western Anatolia, Turkey), J. Volcan. Geother. Res. 115 (2002) 487–510.

[100] T. Emre, H. Sözbilir, Geology, geochemistry and geochronology of the Baflova andesite, eastern end of the Küçük Menderes Graben, MTA Bull. 131 (2005) 1–19 [English edition].

[101] T. Emre, H. Sözbilir, N. Gökçen, Neogene-Quternary stratigraphy of Kiraz-Beydağ region, Küçük Menderes Graben, West Anatolia, MTA Bull. 132 (2006) 1–32 [in Turkish with English abstract].

[102] P.A. Floyd, P.R. Castillo, Geochemistry and petrogenesis of Jurassic ocean crust basalts, ODP leg 129, Site 801. in: *Proceedings of ODP, Scientific Results 129*, Larsen R. *et al*. (eds.), College Station, Texas, 1992, pp. 361–388.

[103] J.A., Winchester, C.R. van Staal, J.P. Langton, The Ordovician volcanics of the Elmtree-Belledune inlier and their relationships to volcanics of the northern Miramichi Highlands, New Brunswick, Canadian J. Earth Sci. 29 (1992) 1430–1447.

[104] K.G. Cox, J.D. Bell, R.J. Pankhurst, *The Interpretation of Igneous Rocks*. London. Allen & Unwin, 1979, 450 p.

[105] J.A. Winchester, P.A. Floyd, Geochemical discrimination of different magma series and their differentiation products using immobile elements, Chem. Geol. 20 (1977) 325–343.

[106] T.N. Irvine, W.R.A. Baragar, A guide to the chemical classification of the common rocks, Canadian J. Earth Sci. 8 (1971) 523–548.

[107] A. Peccerillo, S.R. Taylor, Geochemistry of Eocene calc-alkaline volcanic rocks from the Kastamonu area, northern Turkey, Contrib. Miner. Petrol. 58 (1976) 63–81.

[108] J.W. Shervais, Ti–V plots and the petrogenesis of modern ophiolitic lavas, Earth Planet. Sci. Lett. 59 (1982) 101–118.

[109] M. Meschede, A method of discriminating between different types of mid-ocean ridge basalts and continental tholeiites with the Nb-Zr-Y diagram, Chem. Geol. 56 (1986) 207–218.

[110] P.R. Renne, C.C. Swisher, A.L. Deino, D.B. Karner, T.L. Owens, D.J. De Paolo, Intercalibration of standards, absolute ages and uncertainties in ^{40}Ar/^{39}Ar dating, Chem. Geol. 145 (1998) 117–152.

[111] G. Ruffet, G. Féraud, M. Balèvre, J.-R. Kiénast, Plateau ages and excess argon in phengites: an ^{40}Ar-^{39}Ar laser probe study of Alpine micas (Sesia Zone, Western Alps, northern Italy), Chem. Geol. (Isotopic Geoscience Section) 121 (1995)327–343.

[112] G. Ruffet, G. Gruau, M. Ballèvre, G. Féraud, P. Philippot, Rb-Sr and ^{40}Ar-^{39}Ar laser probe dating of high-pressure phengites from the Sesia zone (western Alps): underscoring of excess argon and new age constraints on the high-pressure metamorphism, Chem. Geol. 141 (1997) 1–18.

[113] J. Keller, Potassic lavas in the orogenic volcanism of the Mediterranean area, J. Volcan. Geother. Res. 18 (1983)321–335.

[114] A.A. Barka, The North Anatolian Fault zone, Annales Tecton. 6 (1992) 164–195.

[115] A. Tankut, M. Wilson, T. Yihunie, Geochemistry and tectonic setting of Tertiary volcanism in the Güvem area, Anatolia, Turkey, J. Volcan. Geother. Res. 85 (1998) 285–301.

[116] R.H. Steiger, E. Jäger, Subcommision on geochronology: convention on the use of decay constants in geo- and cosmo-chronology, Earth Planet. Sci. Let. 36 (1977) 359–362.